CONTENTS

Aims and scope

Building Materials and Structures aims at providing an international forum for communication and dissemination of innovative research and application in the field of building materials and structures. Journal publishes papers on the characterization of building materials properties, their technologies and modeling. In the area of structural engineering Journal publishes papers dealing with new developments in application of structural mechanics principles and digital technologies for the analysis and design of structures, as well as on the application and skillful use of novel building materials and technologies.

The scope of Building Materials and Structures encompasses, but is not restricted to, the following areas: conventional and non-conventional building materials, recycled materials, smart materials such as nanomaterials and bio-inspired materials, infrastructure engineering, earthquake engineering, wind engineering, fire engineering, blast engineering, structural reliability and integrity, life cycle assessment, structural optimization, structural health monitoring, digital design methods, data-driven analysis methods, experimental methods, performance-based design, innovative construction technologies, and value engineering.

Original scientific paper

An experimental study on modification of pervious concrete properties using polyacrylamide

Madhavan Abhinaya[1)], Rangasamy Parthiban[*2)], Naganathan Sivakumar[3)]

[1)] *Department of Chemical Engineering, Sri Sivasubramaniya Nadar College of Engineering, Chennai, 603110, India. ORCID 0009-0000-2244-5965*
[2)] *Department of Chemical Engineering, Sri Sivasubramaniya Nadar College of Engineering, Chennai, 603110, India. ORCID 0000-0002-8992-5004*
[3)] *Department of Civil Engineering, Sri Sivasubramaniya Nadar College of Engineering, Chennai, 603110, India. ORCID 0000-0001-5041-3637*

ABSTRACT

This study tends to use polyacrylamide (PAM) as a potential cement replacer for the enhancement of pervious concrete properties. The study considers four different replacement percentages and compares them with a zero-percentage replacement mix. The properties that were analysed in the fresh state before hardening include slump value, flow percentage, and fresh density of the mix. The analysis also includes further hardened properties such as water absorption, density, infiltration capacity, porosity, and abrasion resistance In addition, compressive strength under two different curing conditions, namely water curing and air curing. is analysed. Microstructural analysis is further performed using FTIR, XRD, and SEM/EDAX to confirm the experimental analysis. The results indicate a 12% increase in the maximum compressive strength in the mix with 0.5% replacement compared to the reference mix. Strength analysis also reveals that the polymer acts as a retarder. Using PAM to replace cement reduces water absorption, density, porosity, and infiltration capacity. In addition, the water treatment ability of various pervious concrete specimens is also analysed in terms of Total Suspended Solids (TSS), Chemical Oxygen Demand (COD). Total Phosphates (TP), Total Nitrogen (TN), Biochemical Oxygen Demand (BOD) and Total Organic Carbon (TOC). Results show that TP removal was as high as 82.5% in a mix with 2% replacement. Therefore, PAM can be regarded as a potential partial cement replacer in pervious concrete.

1 Introduction

The practice of incorporating polymers into construction materials has been in place for the past few decades. Cement's increased pollution during production and application encourages this practice. In addition, increased demand for construction materials has also encouraged the usage of various Supplementary Cementitious Materials (SCMs) one of which is polymers [1-2].

The polymers used in construction can either be natural polymers like cellulose, chitosan etc., or synthetic polymers. Regardless of the polymer type, numerous studies demonstrate that adding polymer binding properties to cement in the Interfacial Transition Zone (IRZ) improves its mechanical properties [3]. In addition to the enhancement in strength, polymer usage even alters the rheology of cement, consequently affecting the other mechanical and durability properties of various construction materials [4–5]. Construction materials can incorporate polymers in a variety of ways. Some studies use polymers as a partial replacement for binder, while others apply them as surface coatings to strengthen their resistance against changing atmospheric conditions [6]. For instance, Chen et al. (2020) [7] have proposed the use of biopolymer chitosan as an additive to Alkali-activated slag-pervious concrete. Results show that chitosan serves as an effective additive for construction materials. Likewise, many other polymers can potentially improve the properties of construction materials in various aspects. One such polymer is Polyacrylamide (PAM).

Laboratories prepare PAM, a water-soluble polymer with the chemical formula $(CH_2CHCONH_2)n$. Various earlier studies reveal that the use of PAM as an additive or replacement in construction materials is beneficial in various aspects. Zhi et al. (2020) [8] in their study have determined that PAM, when added to concrete, has enhanced the corrosion-inhibitive property of steel. This study showed that the addition of PAM to a simulated solution of concrete

---

* Corresponding author:
  E-mail address: rparthi@gmail.com

enhances the corrosion resistance by forming an adsorptive layer on the steel surface. Another study by Li et al., (2020) [9] shows that adding PAM to mortar can improve its cracking resistance. The study reveals that the key factor for improving cracking resistance is the intermolecular hydrogen bonding between cement and acrylamide. The earlier studies suggest that PAM chemically reacts with the binder material to enhance the properties of concrete, steel, mortar, and other construction materials.

Other than the construction industry, PAM has another application in wastewater treatment. Like every other polymer, the active functional groups in PAM possess chelating ability, aiding in flocculative removal of various contaminants when used in wastewater treatment either individually or in combination with some other component [10–11]. Zhao et al. (2015) [12] used PAM as a draw solute in the forward osmosis process in another study. As a result, wastewater treatment properties, along with improved mechanical stability, make the polymer suitable for pervious concrete.

Pervious concrete is an eco-friendly material that has enormous porosity due to its low quantity of fine aggregates. This concrete finds its application in storm water infiltration and pavements as per the ACI 522, 2010 report [13]. The report further indicates that the nominal infiltration capacity, porosity, and compressive strength of pervious concrete mixes range from 0.14 to 1.22 cm/s, 15 to 35%, and 2.8 to 28 MPa, respectively. Despite the lower load-bearing capacity, the other properties of pervious concrete are quite desirable, thereby finding application in evaporative cooling, vehicular noise management, friction reduction, slope stability, etc. Thus, various methods are adapted for enhancement of the compressive strength of the mix without disrupting its basic properties to a greater extent [14–16]. Pervious concrete is also used for wastewater purification. Various studies show that pervious concrete has the ability to purify wastewater. This property thereby aids in the proper recharge of groundwater while simultaneously maintaining its quality [17–18]. Thus, in a broad sense, this paper aims to utilise PAM in pervious concrete to improve its various properties.

The specific objectives of the study include analysing the effects of replacing cement with Polyacrylamide (PAM) in pervious concrete. Effects on pervious concrete are analysed in terms of fresh (Density and Workability) and hardened concrete properties (Water absorption, density, abrasion resistance, porosity, and infiltration capacity). The effects of alternate curing conditions (water and air) on compressive strengths are analysed after the 7th, 14th, and 28th days of curing. Furthermore, microstructural analysis is performed on dried hydrated cement samples using FTIR (Fourier Transform Infrared Spectroscopy), XRD (X-ray Diffraction), and SEM/EDAX (Scanning Electron Microscopy/Energy Dispersive X-ray Analysis). Water purification ability of various samples is determined considering Total Suspended Solids (TSS), Total Phosphates

(TP), Total Organic Carbon (TOC), Total Nitrates (TN), Chemical Oxygen Demand (COD), and Biochemical Oxygen Demand (BOD) as defining parameters.

2 Materials and Methods

2.1 Material Collection and Analysis

Commercial sources supply PAM, which serves as a substitute for cement. PPC (Portland Pozzolanic Cement), confirming IS 1489 (Part 1):1991 [19], is used as a binder. Test procedures from IS 4031 (Parts 4 and 5): 1988 [20-21] are adapted for confirmation of the basic properties of binder. Earlier studies show that the use of coarse aggregate and binder in the ratio 4:1 gives good compressive strength in comparison to other ratios [22]. The water cement ratio of 0.40 was adapted and maintained constant throughout the study. The coarse aggregates used are blue granite stones of 12mm in uniform size that ensure the development of the required permeability [23]. We use 10% (by weight of binder) of M. sand as the fine aggregate. Both the aggregates are procured commercially and are analysed as per the procedure entitled in IS 2386 (Parts 3 and 4):1963 [24–25] and are found to be in line with the specifications entitled in IS 383:1970 [26]. We use normal tap water that meets the usual IS standards for mixing and curing purposes. The study does not include any admixtures. Table 1 displays the mix ratios for mixes with and without replacement.

2.2 Experimental methodology

A post-basic analysis of material mixes with five different ratios is prepared, out of which one mix stands as a reference with zero percentage replacement. Further, four different mixes with polyacrylamide polymer replacing cement in percentages of 0.5%, 1%, 1.5%, and 2% are adapted.

The mix undergoes analysis for fresh properties, specifically workability and fresh density, prior to hardening. Workability is measured in terms of slump value and flow percentage, adapting standard methodology from IS 1199:1959 [27]. Similarly, fresh density is analysed using the procedure specified in ASTM C 1688 (2014) [28], and values are tabulated.

After analysis of fresh properties, 90 cubic samples of size 100mm are cast for determination of compressive strength. Two different curing conditions, viz, water, and air curing are adapted to analyse the effects of polyacrylamide in both curing conditions. Since the coarse aggregates used have a uniform size of less than 20mm, cubes of 100mm size can be used for the determination of strength as per IS 516:2018 [29]. Compressive strength after curing for 7, 14, and 28 days is analysed for both curing conditions. Strength is analysed using a Universal Testing Machine (UTM) with a model number of TVE-CN-600 made by Hitech India Equipment.

Table 1 Mix ratios for Pervious concrete mixes with and without replacement

S. No.	Sample ID	Cement (kg/m^3)	M-Sand (kg/m^3)	Coarse Aggregate (kg/m^3)	Replacement (kg/m^3)
1	1	370	37	1480	0
2	4A	368.15	37	1480	1.85
3	4B	366.3	37	1480	3.7
4	4C	364.45	37	1480	5.55
5	4D	362.6	37	1480	7.4

The cubes are also tested for other hardened properties, namely density and porosity, adapting the procedures outlined in ASTM C 1754 (2012) [30]. In addition, the water absorption of the cubes is also determined by adapting the procedure from Shah and Pitroda (2014) [31].

The sand blasting technique, as described in IS 9284:1979 [32], determines the durability of the cubic specimens in terms of their resistance to abrasion. Analyses are performed in triplicate to ensure stability in the readings obtained.

The other primary parameter, namely the infiltration capacity of pervious concrete sample, is analysed using the procedure from ASTM C 1701 M-09 [33]. This test is named the modified infiltration capacity test and is specifically performed in laboratory conditions. This analysis requires cylindrical samples of size 100 x 200mm. Samples of the required size are cast using PVC moulds with a height of 220mm. This extension is adapted to ensure the maintenance of a standard head of 10mm as described in Haselbach et al., (2017) [34]. Tests are carried out not before pre-wetting the samples to ensure a similar saturation condition in all the specimens.

After the post infiltration capacity test, the same cylindrical samples are used for the analysis of the wastewater purification capacity of pervious concrete, simulating the infiltration of contaminated rainwater. Wastewater samples are collected from the Effluent Treatment Plant at SSN College of Engineering, Tamil Nādu, India. Samples were collected on three consecutive days and analysed for the parameters COD, TOC, TSS, BOD, TN, and TP. The initial characteristics of the raw wastewater sample were similar for almost all three days, with a negligible difference of ±50 ppm. Raw wastewater characteristics in terms of TSS, TP, TN, BOD, TOC, and COD in mg/l are 115, 85.8, 23.1, 462.63, 261.67, and 833, respectively. In this study, we measure TP, TN, and TSS using a DR-9000 reactor from Hach. A 5-day BOD value is considered here and can be measured using the standard Respirometric method using the BODTrak[TM]II apparatus, whereas the DRB 200 reactor from Hach is used to measure

COD and TOC. Adapting (1) determines the removal efficiency of the mixes.

$$\text{Removal efficiency} = \frac{C_i - C_o}{C_i} \text{ X } 100 \qquad (1)$$

3   Results and Discussions

3.1   Fresh Concrete properties

3.1.1   Workability

Figure 1 shows the variation of slump value and flow percentage with respect to PAM percentage in various pervious concrete specimens. According to Figure 1, the slump value and flow percentage of the reference mix are 90mm and 81.33%, respectively, indicating that the mix has medium workability [35]. All the mixes, irrespective of replacement, have shown a shear slump. Another major observation from the graph is that the variation in workability of the mix is proportional to the variation in PAM percentage, thereby changing the medium-workable mix to a highly workable mix. The variation in flow percentage matches the variation in slump value. While a 0.5% replacement does not significantly increase the flow percentage, a further increase in the polymer percentage improves the flow. The lubricating effect of the polymer contributes to the enhanced workability of the mix. This result is consistent with the reactions of other water-soluble polymers, which typically improve the fluidity of the mix as a whole [36].

3.1.2   Fresh density

Fresh density results denote that an increase in PAM percentage reduces the density of the pervious concrete in its fresh state. This indicates the lubricating effect of the water-soluble polymer, which is responsible for the reduction in bulk density of the concrete specimens as percentage replacement increases [37]. This observation is consistent with the hardened density observation, shown in Figure 2.
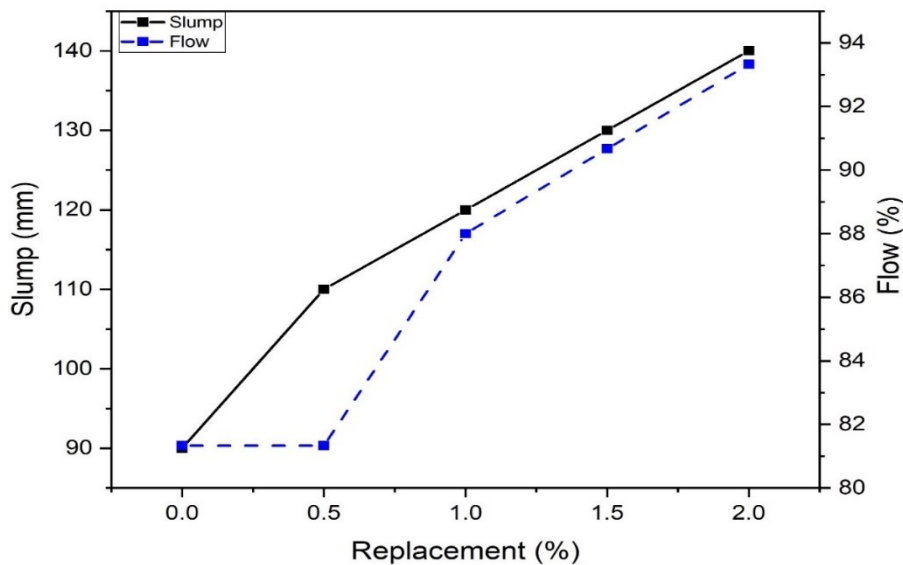
Figure 1. Workability of PAM replaced samples
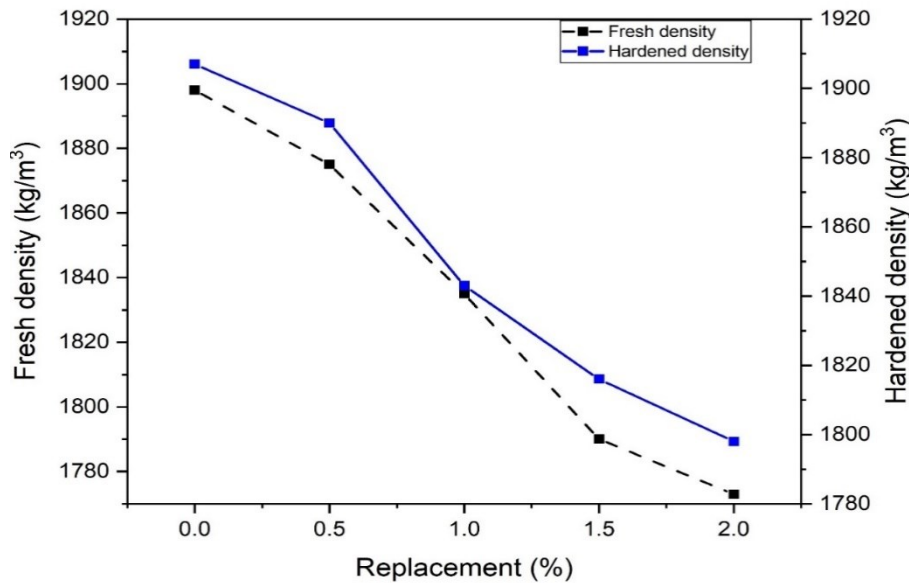
Figure 2. Fresh and hardened density Vs PAM replacement

3.2 Hardened Concrete Properties

3.2.1 Density

Like the fresh density, the hardened density of the mix goes down as the percentage of PAM replacement goes up, as shown in Figure 2. Though hardened density is higher in comparison to fresh density, both follow a similar variation pattern with respect to replacement variation. This slight difference in hardened density from fresh density is nominal, as the variation is less than 2% [38]. Thus, the lubricating and dispersive effects of the water-soluble polymer cause this reduction in density, as discussed in the earlier section.

3.2.2 Porosity

Table 2 shows changes in some hardened properties of pervious concrete mix based on percentage replacement. These properties include water absorption, porosity, percentage abrasion loss, and infiltration capacity. The porosity analysis results show minimal changes in porosity as replacement increases Though the porosity value shows a slight reduction with the increase in replacement for up to 1%, over this level no variation is observed. This is due to the lower percentage of replacement whereas the initial reduction in porosity is mainly due to the dispersion of PAM particles that fill the space amongst coarse aggregates and cement, thereby reducing the porosity of the mix as a whole [39].

3.2.3 Water absorption

Observations from water absorption analyses denote that PAM on replacement tends to reduce the water absorption of the mix. This is because, when cement is replaced with PAM, the polymer particles fill up the minute pores amongst cement and aggregates due to their dispersion properties. This results in a reduction in the free space available for the absorption of water, thereby reducing the water absorption of the mixes [40]. Thus, an increase in the PAM percentage

in pervious concrete reduces the mix's porosity while simultaneously reducing its water absorption. Thus, porosity and water absorption follow almost an inverse relationship with respect to replacement percentage, as shown in Figure 3.

3.2.4 Abrasion resistance

Table 2 displays the percentage abrasion loss for samples with varying PAM percentages. The table reveals that the sample without replacement exhibits a higher percentage loss due to abrasion. The abrasion-induced weight loss of 0.32% exceeds the limits set by IS 9284:1979 for concrete specimens [32]. Still, the mix possesses the eligibility for utilisation in footpaths as per standards. An increase in PAM content enhances the mixes' resistance to abrasion. This abrasion resistance, when correlated with porosity, indicates that a decrease in porosity improves the mix's abrasion resistance. These results are similar to those observed earlier in a study by Muthaiyan and Thirumalai (2017) [41]. The water-soluble and dispersive nature of polymer particles makes it easier for coarse aggregates to stick together. This lowers the porosity, which in turn lowers the weaker areas, making the specimens more resistant to wear.

3.2.5 Infiltration Capacity

From the infiltration capacity results depicted in Table 2, it can be inferred that the specified parameter reduces with every 0.5% increase in PAM percentage. Though the infiltration capacity parameter primarily depends on porosity both do not follow a linear relationship. This is because infiltration capacity, in addition to porosity, also depends on pore connectivity [42]. Thus, the reduction in infiltration capacity is explained by the reduction in pore connectivity as the well-dispersed polymer particles fill the pores in pervious concrete specimens, thereby reducing their corresponding infiltration capacities significantly.
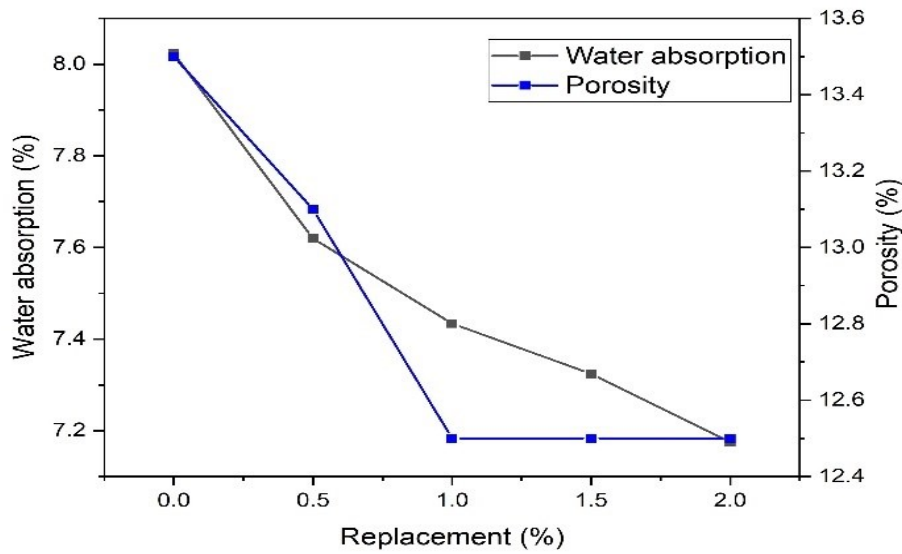
Figure 3. Water absorption and porosity variation with PAM replacement

Table 2. Variation in hardened properties with respect to percentage replacement

S. No.	Replacement (%)	Porosity (%)	Water absorption (%)	Abrasion loss (%)	Infiltration capacity (mm/s)
1	0	13.5	8.023	0.32	7.36
2	0.5	13.1	7.619	0.24	7.35
3	1	12.5	7.434	0.15	5.44
4	1.5	12.5	7.324	0.10	4.62
5	2	12.5	7.175	0.05	4.55

3.2.6   Compressive strength

The effects of PAM on the compressive strength of the sample are analysed under two different curing conditions, namely water curing, and air curing and the readings are tabulated in Table 3. Observations from the results indicate that water curing has a better strength-gaining ability in all samples than air curing, regardless of the replacement percentages. Furthermore, all of the samples show a characteristic increase in strength with respect to curing age.

3.2.6.1   Water curing

When tested after 28 days of curing, samples cured using water according to standard procedures show an increase in strength with a replacement of 0.5% cement. However, a higher number of replacements reduces the strength. PAM on replacement tends to retard the strength-gaining ability of the mix in earlier stages, irrespective of its percentage. This signifies the retarding effect of PAM, which is common for almost all water-soluble polymers [43]. Thus, for all the mixes with PAM strength tested initially, it is low in comparison to the strength of mixes without replacement. However, further curing enhances the strength of the mix with a 0.5% replacement. As the polymer possesses water-retaining ability, it absorbs water, thereby aiding in its hydration. The spread-out polymer particles also help make a membrane around the aggregate particles, which makes it easier for bonds to form in the interfacial transition zone. This aids in an increase in strength [44]. However, despite all the factors, a further increase in PAM reduces the strength since the polymer does not aid in the reduction of porosity as observed

in earlier sections. Thus, with not much change in porosity, the reduction in binder content tends to reduce the strength for replacement by over 0.5%. However, more research is required to understand why the strength decreases by 0.5%.

3.2.6.2   Air curing

Strength development in samples that underwent air curing is lower in comparison to water-cured samples. This is primarily due to a lack of water, which reduces hydration. This decrease in hydration lowers the compressive strength of the samples. Analogous to water curing, air-cured samples also show very low strength in the earlier stage of curing, signifying that PAM serves as a retarder. From the table, it is evident that mixes with PAM replacement possess a lower strength than the reference mix. However, focusing solely on samples containing polymers, we deduce that PAM replacement leads to an increase in compressive strength during air curing. The strength gets better as the PAM percentage goes up. For air-cured samples made with 1.5% PAM replacement, the highest strength was 3.7 MPa. Despite being only 10% higher than the maximum compressive strength in air-cured samples, this result highlights the water absorption and retention abilities of PAM, which contribute to the self-curing of the samples [45]. However, a further increase to 2% results in a very marginal reduction in compressive strength in comparison to the reference mix. This is due to the reduction in binder quantity as well as the reduction in hydration owing to the low quantity of water available for hydration. Thus, the replacement of cement with PAM shows a significant self-curing ability due to the water absorption and retention capacity.

Table 3. Compressive strengths of Pervious concrete samples with PAM replacement

S. No.	Replacement (%)	Compressive strength (MPa)					
		Water curing			Air curing		
		7 days	14 days	28 days	7 days	14 days	28 days
1	0	5.135	6	7.9	2.45	2.98	3.3
2	0.5	4.34	6.06	9	1.64	2.02	2.17
3	1	3.38	4.82	7.7	1.72	1.94	3
4	1.5	2.5	3.64	6.36	2.36	2.52	3.7
5	2	1.8	3.32	4.9	2.54	2.99	3.2

3.3 Micromechanical Analysis

Micromechanical analysis of hydrated cement samples obtained from both curing conditions is performed using FTIR, XRD, and SEM/EDAX. The low replacement percentage explains the lack of remarkable alterations observed for both curing conditions.

3.3.1 FTIR

Figures 4(a) and 4(b) show the variation in FTIR spectra of reference and air-cured samples. As previously discussed, the figures reveal minimal variation in both spectra, with the

(a)

(b)
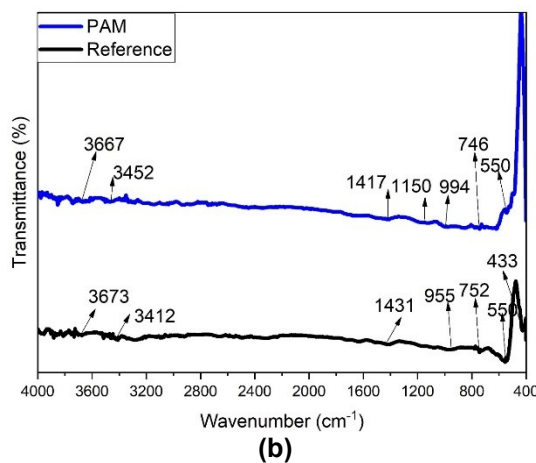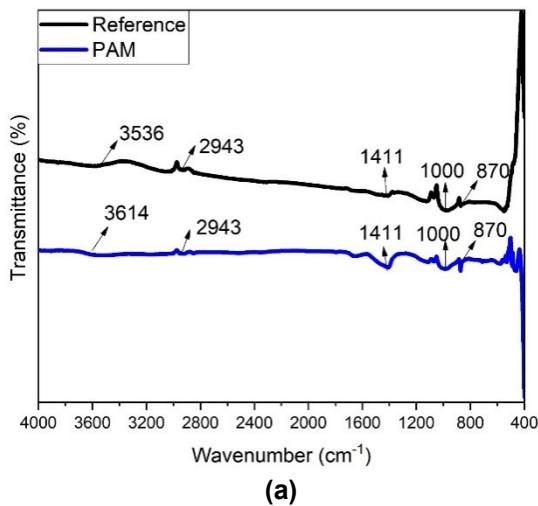
Figure 4. FTIR Spectra of (a) Water cured samples (b) Air cured samples

exception of a few slight shifts and alterations in stretching and bending, due to the lower percentage of replacement. By contrasting the existing peaks in the FTIR spectra of the water- and air-cured reference and PAM mixes, we can observe that all four samples from both curing conditions exhibit similar functional groups. Peaks in the range of 3000 to 4000 cm^{-1} indicate the Hydroxyl group (-OH) which is a characteristic functional group in hydrated cement samples. The presence of hydroxyl groups signifies the hydration of cement after casting pervious concrete samples. In water-cured samples, the peak at 2943 cm^{-1} indicates the presence of a CH bond. Likewise, peaks in the range of 700 to 1500 cm^{-1} signify the presence of alkane and alkyne groups in terms of organic and Si-O, Al-O, and Ca-O when considered in terms of inorganic components. All the bonds signify the presence of Portlandite ($Ca(OH)_2$) and hydrogels (Calcium silicate or Calcium Aluminate (Ca-S-H or Ca-Al-H)), which are characteristic products of hydration obtained from cement. Furthermore, peaks in the range of 400 to 600 cm^{-1} denote the Fe-O functional group, which further indicates the presence of a trace quantity of iron oxide in cement.

3.3.2 XRD

Figures 5(a) and 5(b) show the variation in XRD spectra of water- and air-cured samples, respectively. According to the figures, all four samples in both curing conditions consist of five major components: vizCalcium sulphoaluminate (E - Ettringite), Hydrogel (C-S-H), Calcium hydroxide (P – Portlandite), Calcium Carbonate (C – Calcite) and Silicon dioxide (Q – Quartz) in crystalline phases. In addition, other components are also present, but in trace quantities. In air-cured samples, another crystalline phase observed only in the PAM replaced mix is Aragonite, which is another form of Calcium Carbonate. In the case of air curing, the sample with PAM replacement shows an increase in the intensity of the C-S-H hydrogel peak. This denotes that PAM replacement tends to increase hydration under air curing conditions. In both water- and air-cured conditions, samples with PAM replacement show an increase in calcium carbonate components in various forms. An earlier study by Zhi et al. [46], which observed that PAM addition to cement aids in its carbonation, correlates with this result. These calcite components fill the pores, reducing the mix's porosity and increasing its overall strength. Thus, from the XRD results, it was evident that the usage of PAM as a partial cement replacement enhanced the carbonation and self-curing ability of the pervious concrete.
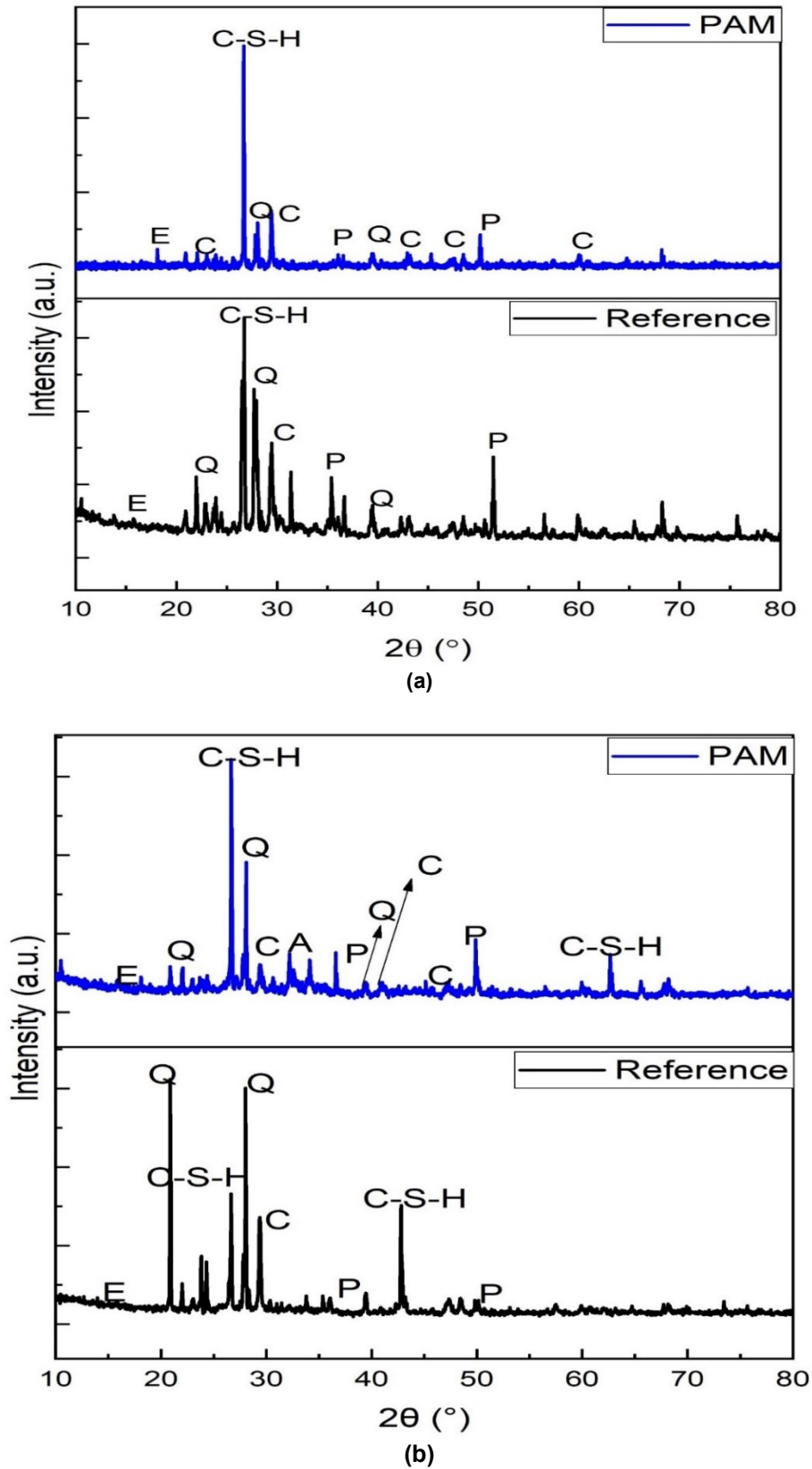
Figure 5. XRD Spectra of (a) Water cured samples (b) Air cured samples

3.3.3 SEM/EDAX

Figures 6 and 7 contrast the SEM/EDAX images of samples with and without PAM replacement in water- and air-cured conditions, respectively. The Figures reveal that the EDAX spectra of all four samples show minimal variation, regardless of the replacement or curing condition. This is due to the lower percentage of replacement. Similarly, SEM images show minimal changes in the microstructure of both the reference and PAM-replaced mix. Both reference and PAM-replaced mixes contain agglomerated patches, which represent calcite and hydrogel. But in the case of PAM, the agglomeration is high in comparison to the reference mix denoting the calcite and hydrogel components, as observed in XRD studies. Ettringite is indicated by the presence of very thin and minute needle structures. SEM images yield little inference other than these minor changes.

SEM images of air-cured samples, as depicted in Figure 7, denote the presence of angular, flaky, and spherical particles. In both cases, we observe little striking variation, except for the shape. This indicates that, with a lower replacement percentage and physical replacement, the internal structure of the mix does not exhibit significant variation. However, further analyses are necessary to confirm this finding.

3.4 Water Purification analysis

The study of wastewater characteristics that leached from the reference pervious concrete specimen itself shows a big drop in the pollutant parameters listed in Table 4. Figure 8 shows how the removal efficiency of different wastewater

parameters changes with the percentage of PAM. Pervious concrete usually eradicates contaminants by means of two different mechanisms, namely microbial degradation and mechanical retention [47]. Mechanical retention is achieved by the chelating property of cement particles. The pores in pervious concrete, on the other hand, hold microbes, which makes the water treatment process more effective. In typical wastewater treatment plants, TSS is removed through filtration. Retention and various other chemical treatments achieve COD reductions, while microbial activity primarily drives BOD and TOC reductions. Chemical and biological processes remove the other two contaminants, TP and TN. According to the study, an increase in PAM content significantly reduces pollution parameters. The maximum removal is observed in 2% replacement. While additional replacement could potentially boost purification efficiency, we discourage it as it could compromise the mix's mechanical performance.

This study shows that the reference mix significantly reduces TSS removal compared to other PAM-replaced mixes. This is due to the enormous porosity of the mix in comparison to PAM-replaced mixes. The pores present in the reference mix have a larger size than TSS particles. Thus, the reference mix shows a removal efficiency of only 9.6% with respect to TSS particles. However, an increase in PAM content fills the voids amongst coarse aggregates, enhancing its ability to retain TSS particles passing through it. Thus, TSS in the resultant leachate is lower than its initial concentration. With the increase in PAM content, there is a significant blockage in pores, thereby increasing TSS removal.
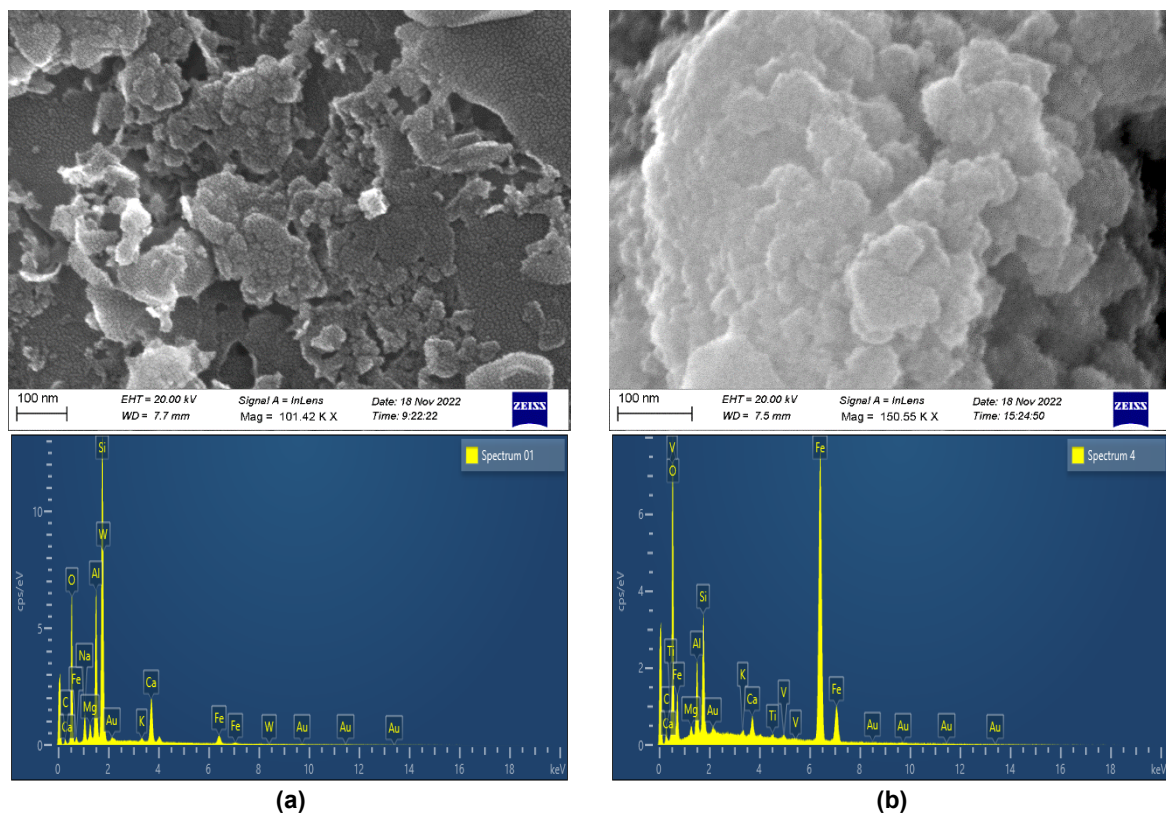
Figure 6. SEM/EDAX of water cured (a) Reference (b) PAM replaced mix
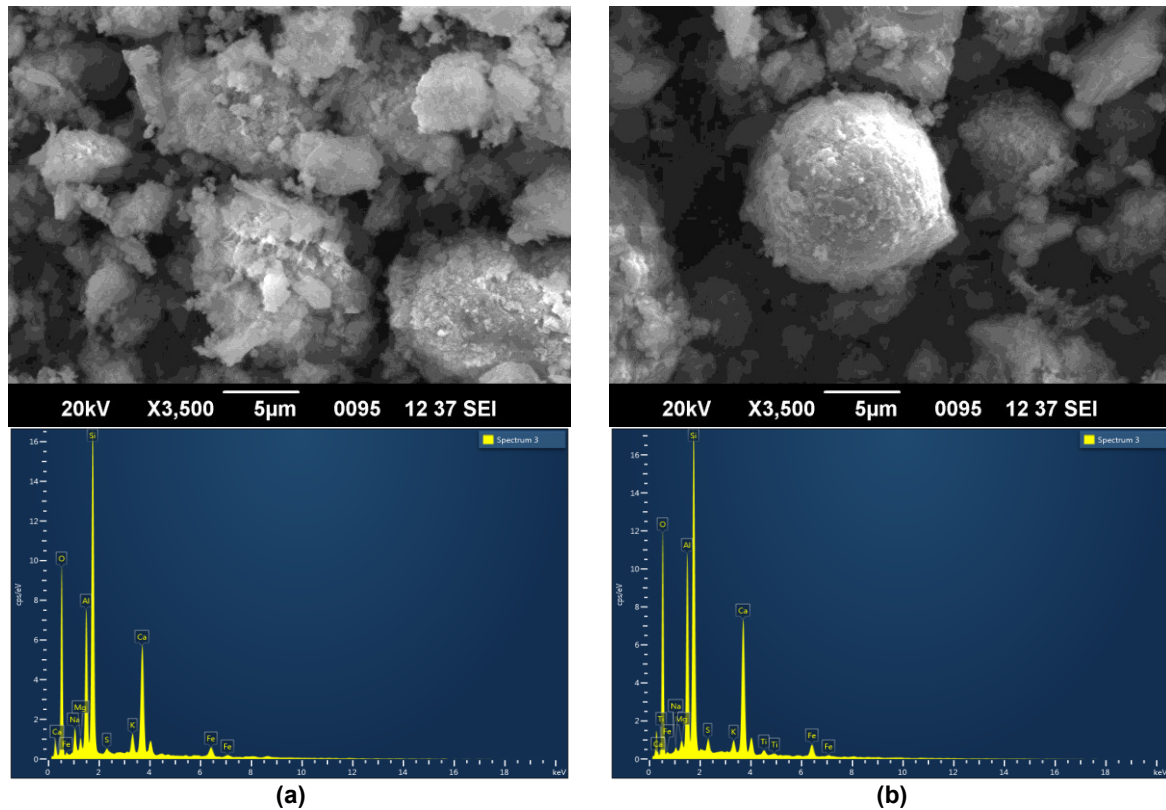
Figure 7. SEM/EDAX of air cured (a) Reference (b) PAM replaced mix

In comparison to all the parameters, TP shows a higher removal rate of 82.5% when the percentage replacement is 2%. TN demonstrates a maximum efficiency of 71.9%, surpassing other parameters, as depicted in Figure. Removal of TP and TN takes place both by mechanical retention as well as microbial degradation remove TP and TN from pervious concrete. In addition, according to reports from earlier studies, the amine groups of the polymer have the ability to adsorb phosphate ions, thereby increasing the overall removal efficiency of phosphate ions [48]. Nitrate also follows a similar mechanism of mechanical retention and microbial degradation with respect to removal. Though in both cases, with the reduction in porosity, there can be a reduction in microbial degradation. Mechanical retentive ability and the presence of polyacrylamide balance this backlog, thereby enhancing the removal efficiency of the mix with respect to phosphate and nitrate.

The parameters COD, BOD, and TOC have almost comparable reduction efficiency, with the maximum being 67.6%, 65.4%, and 64.5%, respectively, for 2% replacement. This reduction in all three parameters can be explained by mechanical retention as well as microbial degradation, as mentioned earlier. While the increase in PAM ensures an enhancement in retention, signifying an increase in the rate

of COD removal in comparison to BOD and TOC. This also explains the lower COD removal in the reference pervious concrete specimen compared to the PAM-replaced mix. The addition of PAM enhances the possibility of chelating inorganic contaminants, while simultaneously reducing porosity. This reduction in porosity reduces microbial proliferation, resulting in a higher rate of COD reduction compared to BOD and TOC, as shown in Figure. On the other hand, despite the reduction in pores, there is an enhancement in BOD and TOC removal. This also indicates the chelating ability of amine functional groups in PAM polymers, which retain both organic and inorganic contaminants. The increase in retention time is another significant factor that aids in the reduction of these parameters. With the increase in PAM, there is a reduction in the infiltration rate of water through every sample. This lessening of infiltration increases the time that wastewater is in contact with different types of pervious concrete, which mechanically retains a lot of the contaminants. However, more research is necessary to confirm the combined efficiency of wastewater treatment using PAM instead of Pervious concrete mixes, as there are not many studies available elsewhere in this area.

Table 4. Characteristics of Wastewater post passing through Pervious Concrete

S. No.	Replacement (%)	TSS (mg/l)	TP (mg/l)	TN (mg/l)	BOD (mg/l)	TOC (mg/l)	COD (mg/l)
1	0	104	35	17	288.63	170	558
2	0.5	77	30	14.5	225	136.9	400
3	1	69	21	11	200	117	346
4	1.5	57	17.7	9.5	180.07	105	307
5	2	51	15	6.5	160	93	270
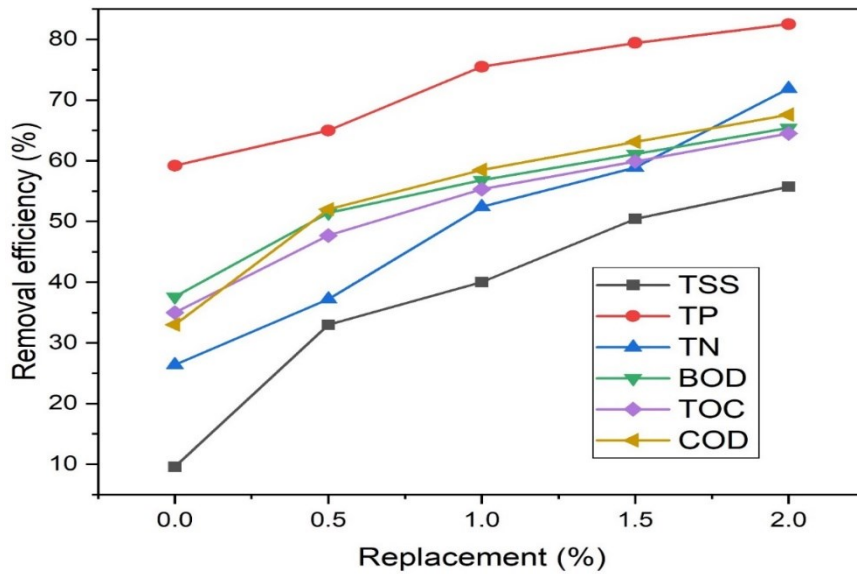
Figure 8. Removal efficiency Vs Percentage Replacement using PAM

4 Conclusion

Water-soluble polymers are used to partially replace cement in pervious concrete. Polyacrylamide significantly alters the engineering properties of concrete. Polymer replacement seemingly enhances the workability and converts the medium workable mix to a highly workable one. This is due to the water-soluble nature of the polymer, which enhances the fluidity of the mix. The same lubricating effect of the polymer reduces the fresh and hardened density of the mix. Furthermore, an increase in percentage replacement significantly reduces the specimens' porosity, water absorption, and infiltration capacity. Furthermore, the dispersive nature of the polymer explains the increase in resistance to abrasion as the PAM percentage increases.

The results of compressive strength analysis under water curing conditions indicate that when PAM is replaced for up to 0.5%, it increases in strength. Further enhancement decreases strength. Increased Porosity up to 1% does not significantly impact compressive strength. The reduction in binder content primarily explains this phenomenon. This study demonstrates that compressive strength not only depends on physical factors like density and porosity, but also on a chemical factor, namely binder content. To some extent, a reduction in binder content does not affect compressive strength. However, further reduction in the binder content tends to reduce the compressive strength despite the increase in porosity of the mix.

It is also observed that PAM serves as a retarder, thereby reducing the mechanical efficiency of the mix during the initial curing period. In the case of atmospheric curing, it is inferred that PAM serves as a self-curing agent. Micromechanical analysis by XRD further confirms these results, indicating the enhanced hydration of the mix through variations in intensity and peaks. FTIR and SEM/EDAX results show no significant variation owing to the lower replacement percentage.

Water purification analysis results reveal that inculcation of PAM into pervious concrete mix enhances the water purification ability significantly. With respect to all parameters, 2% replacement showed the maximum reduction efficiency. Of all the parameters considered, TP showed the maximum removal, whereas TSS showed the minimum one. The primary mechanisms involved in water purification are mechanical retention and microbial degradation. PAM replacement improves the samples' mechanical retention ability.

Thus, on a concluding note, it can be said that PAM serves as a potential alternate for cement in pervious concrete when used in a limited quantity. While a 2% replacement is optimal for water purification, we limit the replacement percentage to 0.5% or 1% to avoid compromising other pervious concrete efficiencies. Hence, according to ACI reports, PAM-replaced concrete serves as a cleaner alternative for its use in sludge drying beds, considering its water purification ability as a characteristic parameter.

CRediT author contribution

M Abhinaya: Methodology, Investigation, Writing – Original draft

R. Parthiban: Conceptualization, Supervision, Writing – Review & Editing

N. Sivakumar: Methodology, Writing – Review & Editing, Validation

Declaration of Competing Interests

The authors have no relevant financial or non-financial interests to disclose.

Acknowledgements

References

[1] C. Kiruthika, S.L. Prabha, M. Neelamegam, Different aspects of polyester polymer concrete for sustainable construction. Mater. Today Proc. 43 (2021), 1622-1625.

[2] N. Poornima, D. Katyal, T. Revathi, M. Sivasakthi, R. Jeyalakshmi, Effect of curing on mechanical strength and microstructure of fly ash blend GGBS geopolymer, Portland cement mortar and its behaviour at elevated temperature. Mater. Today Proc. 47 (2021), 863-870.

[3] U.T. Bezerra, R.M. Ferreira, J.P. Castro-Gomes, The effect of latex and chitosan biopolymer on concrete properties and performance. Key Eng. Mater. 466 (2011), 37-46.

[4] H. Yao, M. Fan, T. Huang, Q. Yuan, Z. Xie, Z. Chen, Y. Li, J. Wang, Retardation, and bridging effect of anionic polyacrylamide in cement paste and its relationship with early properties. Constr. Build. Mater. 306 (2021), 124822.

[5] H. Bessaies-Bey, R. Baumann, M. Schmitz, M. Radler, N. Roussel, Effect of polyacrylamide on rheology of fresh cement pastes. Cem. Concr. Res. 76 (2015), 98-106.

[6] R. Aguilar, J. Nakamatsu, E. Ramirez, M. Elgegren, J. Ayarza, S. Kim, M.A. Pando, L. Ortega-San-Martin, The potential use of chitosan as a biopolymer additive for enhanced mechanical properties and water resistance of earthern construction. Constr. Build. Mater. 114 (2016), 625-637.

[7] X. Chen, Z. Niu, H. Zhang, M. Lu, Y. Lu, M. Zhou, B. Li, Design of a chitosan modifying alkali-activated slag pervious concrete with the function of water purification. Constr. Build. Mater. 251 (2020), 118979.

[8] F. Zhi, L. Jiang, M. Jin, P. Xu, B. Xiao, Q. Jiang, L. Chen, Y. Gu, Inhibition effect and mechanism of polyacrylamide for steel corrosion simulated concrete pore solution. Constr. Build. Mater. 259 (2020), 120425.

[9] H. Li, D. Ni, L. Li, B. Dong, Q. Chen, L. Gu, Insight into the role of polyacrylamide polymer powder on the cracking in plastic period of cement mortar. Constr. Build. Mater. 260 (2020), 119914.

[10] S.S. Wong, T.T. Teng, A.L. Ahmad, A. Zuhairi, G. Najafpour, Treatment of pulp and paper mill wastewater by polyacrylamide (PAM) in polymer induced flocculation. J. Hazard. Mater. B135 (2006), 378-388.

[11] Q. Chang, X. Hao, L. Duan, Synthesis of crosslinked starch-graft-polyacrylamide-co-sodium xanthate and its performances in wastewater treatment. J. Hazard. Mater. 159 (2008), 548-553.

[12] P. Zhao, B. Gao, S. Xu, J. Kong, D. Ma, H.K. Shon, Q. Yue, P. Liu, Polyelectrolyte-promoted forward osmosis process for dye wastewater treatment – Exploring the feasibility of using polyacrylamide as draw solute. Chem. Eng. J. 264 (2015), 32-38.

[13] ACI. 522R-10, Report on Pervious Concrete ACI Committee, 522, 2010, p. 38.

[14] O. Alshareedah, S. Nassiri, Pervious concrete mixture optimization, physical and mechanical properties, and pavement design: A review. J. Clean. Prod. 288 (2021), 125095.

[15] A.K. Chandrappa, K.P. Bilgiri, Pervious concrete as a sustainable pavement material – Research findings and future prospects: A-state-of-the-art review. Constr. Build. Mater. 111 (2016), 262-274.

[16] S.K. Ghosh, A. Chaudhury, R. Datta, D.K. Bera, A review on performance of pervious concrete using waste materials. Int. J. Res. Eng. Tech. 4 (2015), 105-115.

[17] M.J. Lee, M.G. Lee, Y. Huang, C.L. Chiang, Purification study of pervious concrete pavement. Int. J. Eng. Technol. 5 (2013), 532-535.

[18] M.G. Lee, M. Tia, S.H. Chuang, Y. Huang, C.L. Chiang, Pollution, and purification Study of the Pervious Concrete Pavement Material. J. Mater. Civ. Eng. 26 (2014), 04014035.

[19] IS 1489 (Part 1): 1991. Portland-Pozzolana cement specification. Fly Ash based. Bureau of Indian standards. New Delhi.

[20] IS 4031 (part 4): 1988. Methods of physical tests for hydraulic cement. Determination of consistency of standard cement paste. Bureau of Indian standards. New Delhi.

[21] IS 4031 (part 5): 1988. Methods of physical tests for hydraulic cement. Determination of initial and final setting times. Bureau of Indian standards. New Delhi.

[22] D.P.M. Tripathi, S.M.A. Hussain, P. Madhav, An Experimental Study on Pervious Concrete (Mix-Ratio, Strength, and Porous Properties). Int. J. Eng. Res. Tech. 6 (2017), 100-103.

[23] M. Sonebi, M. Bassuoni, A. Yahia, Pervious Concrete: Mix Design, Properties and Applications. RILEM Tech. Lett. 1 (2016), 109-115.

[24] IS 2386 (part 3):1963. Methods of test for aggregates of concrete. Specific gravity, Density, voids absorption and bulking. Bureau of Indian standards. New Delhi.

[25] IS 2386 (part 4):1963. Methods of test for aggregates of concrete. Mechanical properties. Bureau of Indian standards. New Delhi.

[26] IS 383:1970. Specification for coarse and fine aggregates from natural sources of concrete. Bureau of Indian standards. New Delhi.

[27] IS 1199:1959. Methods of sampling and analysis of concrete. Bureau of Indian standards. New Delhi.

[28] ASTM C1688/C1688M-2014. Standard Test Method for Density and Void Content of Freshly mixed Pervious Concrete, ASTM International, West Conshohocken. PA.

[29] IS 516:2018. Methods of tests for strength of concrete. Bureau of Indian standards. New Delhi.

[30] ASTM C1754/C1754M-2012. Standard Test Method for Density and Air Void Content of Pervious Concrete, ASTM International, West Conshohocken, PA.

[31] D.S. Shah, J. Pitroda, An experimental study on durability and water absorption properties of pervious concrete. Int. J. Res. Eng. Technol. 3 (2014), 439-444.

[32] IS 9284:1979. Methods of Test for Abrasion Resistance of Concrete. Bureau of Indian standards. New Delhi.

[33] ASTM C 1701/C1701 M-2009. Standard Test Method for Infiltration Rate of In place Pervious Concrete, ASTM International, West Conshohocken, PA.

[34] L. Haselbach, B. Werner, V.P. Dutra, P. Schwetz, L.C. Pinto da Silva Filho, R. Batezini, F. Curvo, J.T. Balbo, Estimating porosity of In Situ Pervious Concrete using Surface Infiltration Tests. J. Test. Eval. 45 (2017), 1726-1735.

[35] A.M. Neville, Properties of concrete. 5th edition, Longman, England, 2011.

[36] Q. Yuan, Z. Xie, H. Yao, M. Fan, T. Huang, Comparative studies on early properties of cement modified with different ionic polyacrylamides. Constr. Build. Mater. 339 (2022), 127671.

[37] A.M. Hameed, R.R.Rawdhan, S.A. Al-Mishhadani, Effect of self-curing agents on the different properties of cement and mortar. Int. J. Curr. Res. 9 (2017), 54586-54594.

[38] M. Rangelov, S. Nassiri, Z. Chen, M. Russell, J. Uhlmeyer, Quality evaluation tests for pervious concrete pavements' placement. Int. J. Pavement Res. Technol. 10 (2017), 245-253.

[39] B. Bose, C.R. Davis, K.A. Erk, Microstructural refinement of cement paste internally cured by polyacrylamide composite hydrogel particles containing silica fume and nano silica. Cem. Concr. Res. 143 (2021), 106400.

[40] U.S. Rai, R.K. Singh, Effect of polyacrylamide in the different properties of cement and mortar. Mat. Sci. Eng. A. 392 (2005), 42-50.

[41] U.M. Muthaiyan, S. Thirumalai, Studies on the properties of pervious fly ash-cement concrete as a pavement material. Cogent Eng. 4 (2017), 1318802.

[42] R. Selvaraj, M. Amirthavarshini, Some aspects on Pervious concrete. Int. J. Eng. Appl. Sci. 3 (2016), 6-10.

[43] P.C. Mishra, V.K. Singh, K.K. Narang, N.K. Singh, Effect of carboxymethyl-cellulose on the properties of cement. Mat. Sci. Eng. A. 357 (2003), 13-19.

[44] P. Shen, J.-X. Lu, H. Zheng, S. Liu, C.S. Poon, Conceptual design and performance evaluation of high strength pervious concrete. Constr. Build. Mater. 269 (2021), 121342.

[45] A.S. El-Dieb, T.A. El-Maaddawy, A.A.M. Mahmoud, Water soluble polymers as self-curing agents in cement mixes. Adv. Cem. Res. 24 (2012), 291-299.

[46] F. Zhi, Y. Jiang, M.Z. Guo, X. Jin, X. Yan, P. Zhu, L. Jiang, Effect of polyacrylamide on the carbonation behaviour of cement paste. Cem. Concr. Compos. 156 (2022), 106756.

[47] C. Xie., L. Yuan, H. Tan, Y. Zhang, M. Zhao, Y. Jia, Experimental study on the water purification performance of biochar-modified pervious concrete. Constr. Build. Mater. 285 (2021), 122767.

[48] Y.-F. Lin, H.-W. Chen, Y.-C. Chen, C.S. Chiou, Application of magnetite modified with polyacrylamide to adsorb phosphate in aqueous solution. J. Taiwan Inst. Chem. Eng. 44 (2013), 45-51.

Građevinski materijali i konstrukcije
Building Materials and Structures

journal homepage: www.dimk.rs

Original scientific paper

Study on the mechanical property, water absorption, and acid resisitance of steel and polypropylene hybrid fiber reinforced recycled aggregate concrete

Vijayalakshmi Ramalingam*1), Javith Shainsha2), Madhuru Harshitha3), Oshiyana Ramadoss4)

4) Associate Professor, Department of Civil Engineering, Sri Sivasubramaniya Nadar College of Engineering, Kalavakkam Chennai-603110, Tamil Nadu, India. ORCID 0000-0003-4678-2020
5) Under graduate Students, Department of Civil Engineering, Sri Sivasubramaniya Nadar College of Engineering, Kalavakkam Chennai-603110, Tamil Nadu, India. ORCID 0009-0002-1897-7744
6) Under graduate Students, Department of Civil Engineering, Sri Sivasubramaniya Nadar College of Engineering, Kalavakkam Chennai-603110, Tamil Nadu, India. ORCID 0009-0005-0031-2199
7) Under graduate Students, Department of Civil Engineering, Sri Sivasubramaniya Nadar College of Engineering, Kalavakkam Chennai-603110, Tamil Nadu, India. ORCID 0009-0005-2099-5468

ABSTRACT

This study aims to develop a sustainable solution in the construction industry by incorporating recycled aggregate (RA) into concrete, partially replacing natural gravel aggregate, and enhancing the strength of RA concrete through the addition of hybrid s The study investigates the effect of steel and polypropylene hybrid s on the mechanical and durability properties of recycled aggregate concrete (RAC). The research was carried out in three phases/mixes. The first mix is with different proportions of recycled aggregate (25% and 50%). The second mix is recycled aggregate concrete with only macro-steel , and the third mix is recycled aggregate concrete with different proportions of macro-steel and micro-polypropylene . Mechanical and durability properties were investigated in all three types of concrete mixes and compared with the control mix. The study concluded that the mechanical properties of hybrid fiber reinforced recycled aggregate concrete (HFRRAC) are dependent on the amount of recycled aggregate, proportions, and type. The macro-steel fibers with high elasticity modulus and stiffness improve the concrete´s strength and toughness. The increase in content affects the workability of -reinforced concrete. Synthetic microfibers with excellent ductility and dispersion improve concrete's mechanical properties and durability. Synthetic microfibers when used along with macro-steel improve both mechanical properties and durability characteristics.

1 Introduction

Urbanisation results in the construction of numerous new buildings and the demolition of old ones, leading to a significant build-up of construction and demolition waste [1]. Utilizing such waste concrete material into the concrete mainly reduces the consumption of natural aggregate and reduces land pollution. Replacing the coarse gravel aggregates which are the major ingredient in the concrete, with recycled aggregate (RA), may lead to a sustainable concrete solution [2]. Recycled aggregates, primarily used in the construction of non-structural members and for foundation filling, are often considered inferior to gravel aggregate. To change this idea, a lot of research is being carried out using RA, and investigations are being carried out to study the mechanical and durability properties of such recycled aggregate concrete (RAC) [3]. Researchers have reported that RA influences the major strength properties of

concrete, exhibiting increased peak strain and a decrease in the modulus of elasticity under compression load [4]. Cement matrix, which is attached to the old aggregates, has an influence on the strength of concrete [5]. Thus, the proportions, aggregate type, amount of impurity, and other parameters influence the behaviour of recycled aggregate concrete.

To enhance the properties of recycled aggregate concrete, different types of fibers are added to the concrete to improve its strength, fracture behavior, and impact resistance [6]. The addition of macro-steel fibers in concrete improves the tensile property of concrete and the post-cracking behaviour [7]. The macro-steel fiber plays a major role after the appearance of the first crack in concrete and prolongs the ultimate failure of the structure [8]. The volume fraction, length of steel , and pattern of steel influence the performance of concrete [9], [10], [11], [12], and [13]. Studies seem to suggest that the compressive strength of macro-

* Corresponding author:
E-mail address: vijayalakshmir@ssn.edu.in

steel FRC increases by up to 10% when compared to plain concrete. Furthermore, the failure mode of macro-steel FRC transitions from brittle to ductile, resulting in a significant improvement in the post-cracking response [14]. These days, the light weight, chemical resistance, and high strength-to-weight ratio of micro-polypropylene fibers make them a popular choice for microfiber reinforcement. Micro-polypropylene fibers also improve the tensile property of plain concrete, showing high resistance to impact loads and better fracture behaviour [15], [16], and [17]. Today, concrete incorporates various natural fibers like jute, bamboo, banana, sisal, and caryota fibers [18] [19] [20] [21] as well as synthetic fibers like steel, polypropylene, plastic, glass, and basalt fibres [8] [22] [23] [24]. These fibers are used as monotype fibers or in combination as hybrid fibers. Popularly, macro-steel and micro-polypropylene fibers are used in combination as hybrid fibers. Macro steel fibers as a macro-scale reinforcement with a high Young's modulus are highly efficient in bridging the critical macro-cracks and improves the strength of concrete, and micro polypropylene fiber, as a micro-scale reinforcement, could reduce the plastic shrinkage cracks in the early age of concrete and enhance the post-cracking behavior [14], [25], and [26]. Based on the multiscale crack behaviour of concrete, it will be more advantageous to use both micro and macro fibers as hybrid reinforcement, which arrests cracks at micro and macro level. Hybrid fiber reinforcement also plays a major role in arresting the early stage shrinkage crack and post cracking behaviour of concrete [27].

As a result, blending two types of s in the concrete matrix appears to be more effective in crack arrest at multiple levels. The literature review revealed that numerous studies have examined the mechanical characteristics of recycled aggregate concrete reinforced with single and hybrid s. But an optimum proportion for hybrid fiber content is yet to be obtained. Therefore, the main objective of this research work is to study the mechanical behavior of recycled aggregate concrete with macro-steel fibers and micro polypropylene s. Mechanical properties such as compressive strength, tensile strength, and flexural properties, as well as durability properties such as water absorption and acid resistance, are to be studied in detail.

2 Experimental Investigation

2.1 Material characterization

The control concrete mix was prepared using ordinary Portland cement (specific gravity SG = 3.15 g/cm^3), lime stone gravel aggregate of size 10 mm used as coarse aggregate (CA), and recycled aggregate (RA) of size 18-20 mm used as a partial replacement for coarse aggregate. and river sand (SG = 2.74 g/cm^3) used as fine aggregate. To produce hybrid fiber reinforced recycled aggregate concrete, macro steel and micro polypropylene fiber were used in different proportions in addition to the above ingredients. The scanning electron microscope (SEM) image showing the detailed structure of macro-steel and micro-polypropylene is shown in Figure 1. The micro-polypropylene and macro-steel used in the present experimental investigation are shown in Figure 2. The physical properties of macro steel s and micro-polypropylene are listed in Tables 1 and 2, respectively.
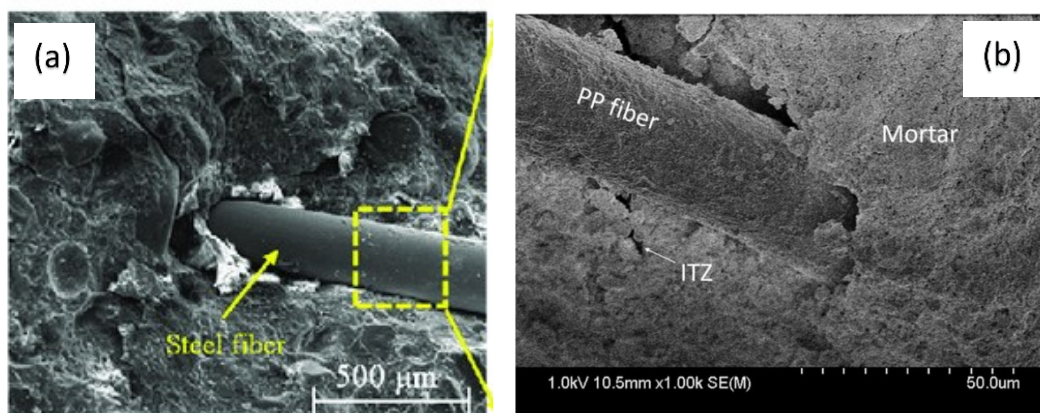
Figure 1. (a) SEM image: (a) Macro-steel fiber [28] (b) Micro-Polypropylene fiber [29] in concrete matrix
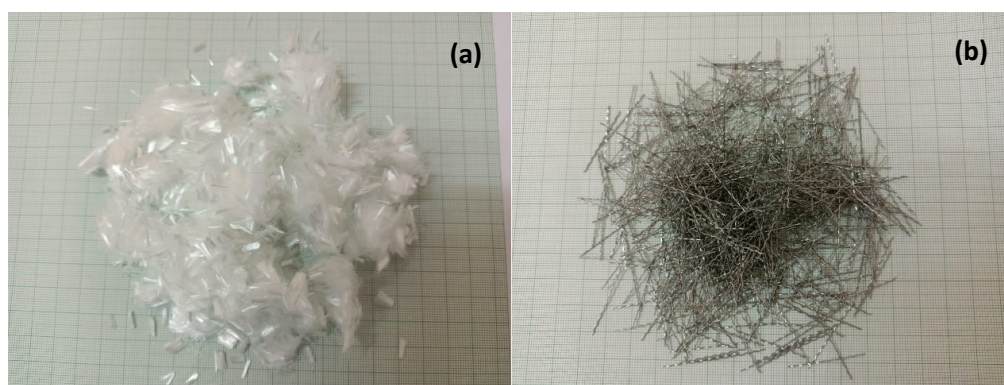
Figure 2. (a) Micro-Polypropylene fiber (b) Macro-Steel Fiber

Table 1. Physical property of macro steel fiber

Physical property	Range
Shape	Crimped steel fiber
Length (mm)	25
Diameter (mm)	0.5
Aspect Ratio (l/d)	50
Tensile Strength (MPa)	2650
Unit Weight (g/cm^3)	7.85
Coating	None
Elastic Modulus, (GPa)	200

Table 2. Physical property of micro-polypropylene fiber

Physical property	Range
Raw material	100 % polypropylene
Type	monofilament
Length	4-5 mm
Diameter	30-40μm
Melting point	105±10°C
Softening point	95±10°C
Acid & alkaline resistance	Strong
Density	0.91 g/cm3
Colour	white
Water absorption	No
Specific Gravity	0.9
Youngs modulus	3.45 ×10^{3}Mpa
Tensile Strength	551 Mpa

2.2 Mix proportions and specimen ID

The concrete ingredients for the control mix, namely the cement, sand, coarse aggregate, water, and plasticizer, were mixed in the proportion of 1:1.64:1.72: 0.32: 0.01. The mix for concrete mortar cubes was done using a concrete mixer.

Normal concrete cement of 19.8 kg fine aggregate of 30.15 kg, and coarse aggregate of 49.14 kg were filled in the mixer. We mixed the dry mixture for approximately one minute. After slowly adding water to the mixer and mixing it for two minutes, we cast the specimens. Fibers were added to the fresh concrete mix, and the concrete was mixed for another minute. Figures 3(a) and 3(b) show the addition of macro-crimped steel and micro-Polypropylene s, respectively. A total of 3 cubes (150 × 150 × 150 mm), 3 cylinders (150 × 300mm) and 3 beams (150 × 150 × 750 mm) were cast for each mix. For the preparation of hybrid fiber-reinforced recycled aggregate concrete, cement, fine, and coarse aggregates are added to the mixer. We added water to the mixture after mixing for 2 minutes. After allowing it to mix for 2 minutes, macro-steel and micro-polypropylene fiber were added to it. Table 3 lists the mix proportions.

2.3 Testing of specimens

According to IS 516:1959, a compression test was carried out on standard 150 mm x 150 mm x 150 mm cube specimens. All the cubes were tested in a surface dried condition, and for each mix combination, three cubes were tested at the age of 28 days using a compression testing machine of 1000 kN capacity. The loading was continued until the specimen reached its ultimate load. The load was applied without shock at a rate of 1.2 kN/m^2. In accordance with IS 516:1959, we conducted a tensile test on a 300 mm by 150 mm cylinder specimen after 28 days. The test was carried out on a universal testing machine of 2000 kN capacity. We calculated the tensile strength from the obtained load using the standard formula. For each mix, three cylinders were tested after 28 days of curing, and the mean value is reported. According to IS 516:1959, a flexural test was carried out on a beam specimen with dimensions of 500mm x 100mm x 100mm at the age of 28 days. A universal testing machine with a 2000 kN capacity conducted the test. Three-point loading was given to the specimens, and the flexural load was recorded at the time of failure. For each mix, three beams were tested after 28 days of curing, and the mean value was tabulated. Figure 4(a–d) displays the casted specimen and the mechanical testing of the specimen.

MacroCrimped Steel Fibers
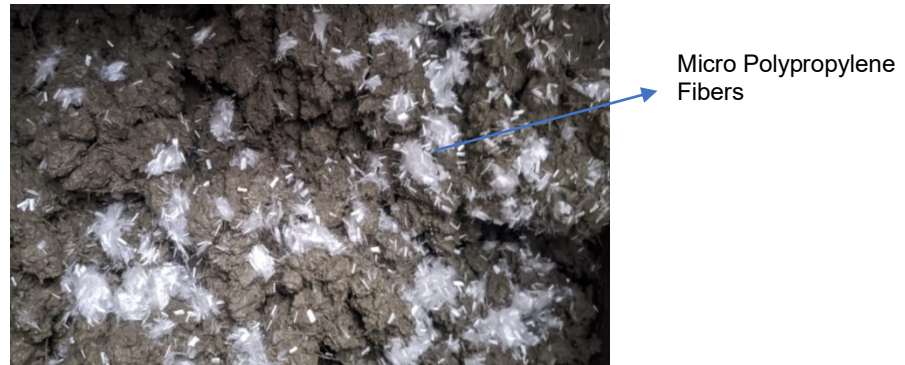
Figure 3. Mixing fibers in fresh concrete mix (a) macro-steel fiber (b) micro-polypropylene fiber

Table 3. Mix proportions

MIX	Cement (kg/m³)	Recycled Aggregate (kg/m³)	Gravel (kg/m³)	Sand (kg/m³)	Water (kg/m³)	Macro Steel fiber (kg/m³)	Micro PP fiber (kg/m³)
Normal mix	790	-	1966	1206	366	-	-
RCA 25	790	437	1474	1206	366	-	-
RCA 25% + SF 0.5%	790	437	1474	1206	366	70.4	-
RCA 25% + 0.75% SF + 0.25% PP	790	437	1474	1206	366	52.8	16
RCA 25% + 1% SF + 0.5%PP	790	437	1474	1206	366	140	70.4
RCA 50%	790	874	983	1206	366	-	-
RCA 50% + SF 0.5%	790	874	983	1206	366	70.4	-
RAC 50% + 0.75% SF + 0.25% PP	790	874	983	1206	366	52.8	16
RCA 50% + 1% SF + 0.5%PP	790	874	983	1206	366	140	70.4
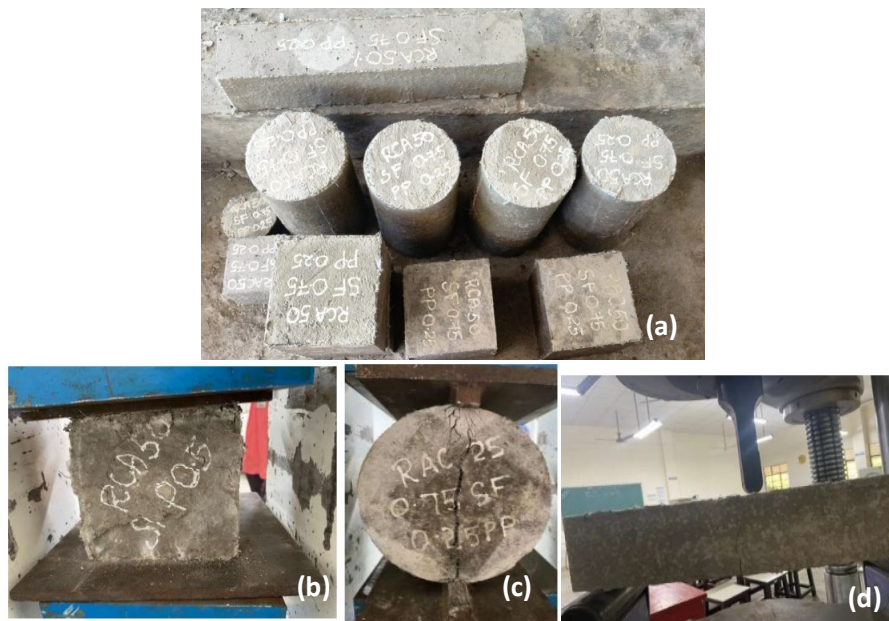
Figure 4(a). Cast specimens and (b-d) testing HFRAC specimens

2.4 Water absorption test

The water absorption test determines the water absorption rate (sorptivity) of both the outer and inner concrete surfaces. The test measures the increase in mass of concrete samples due to water absorption over time, with only one face of the specimen exposed to water. Concrete resistance against the ingress of aggressive ions is one of the major factors from the viewpoint of concrete durability. Water absorption behavior provides useful information about concrete porosity. It depicts the concrete's permeable pore volume as well as its pore connectivity. We dry the specimens in an oven for a specified time and temperature for the water absorption test, and then cool them in a desiccator. Immediately upon cooling, the specimens are weighed. The material is then immersed in water at agreed-upon conditions, often 23 °C for 24 hours or until equilibrium. Figure 5 illustrates the test arrangement for the water absorption test.

2.5 Acid Attack test

Concrete is susceptible to acid attack because of its alkaline nature. The components of the cement paste disintegrate when they come into contact with acids. The decomposition of the concrete depends on the porosity of the cement paste and the attention of the acid, and the solubility of the acid calcium salts (CaX_2). Insoluble calcium salts may percolate in the voids, slowing down the attack. Sulphuric acid interacts with the surface of the concrete, causing it to deteriorate. With the increase in environmental pollution, the rainwater has also become more acidic. Hence, there is a need to study the durability properties of concrete by exposing it to an acidic environment. We cast a 100 x 100 mm cube and cured it in a curing tank for 28 days. Concentrated sulphuric acid was diluted to 1N, and the mould was immersed in a tub containing the sulphuric acid solution shown in Figure 6(a). Initially, the dry weight of the mould was measured. After clearing the cube's surface with a metallic brush on the 3rd, 7th, and 14th days, we recorded the weight, as shown in Figure 6(b). Figure 6 (c-d) displays the cleaned cube specimen that underwent acid immersion for 3 days, 7 days, and 14 days. We tested the cubes under uniaxial compression after the 14th day and recorded the compressive load values.

Figure 5. Water absorption test arrangement for control Mix, RACand HYFRAC specimen

Figure 6(a). Cubes immersed in sulphuric acid (b) removing of loose materials with metal brush (c) Immersed cubes on 3rd day (d) Immersed cubes on 7th day (e) immersed cubes on 14th day

3 Results and Discussion

We conducted an experimental study to investigate the mechanical and durability properties of recycled aggregate concrete and hybrid fiber-reinforced recycled aggregate concrete. We observed mechanical properties such as compressive strength, flexural strength, and tensile strength, and Table 4 tabulates the results.

3.1 Workability of recycled aggregate concrete and hybrid fiber reinforced recycled aggregate concrete

A slump test is frequently used to measure the flow ability of concrete. The slump values dictate how easily the concrete flows and fits into the mould. Table 4 lists the recorded slump value for the current work. Figure 7 illustrates the variation in slump for the control mix using RAC and HFRRAC concrete mixes. Previous research work suggested that the slump of conventional concrete varies from 100 to 125 mm, while that of lightweight aggregate concrete ranges from 50 mm to 75 mm. The control mix recorded a slump value of 83 mm, which decreased as the amount of SF and PP in the concrete increased. With the addition of 25% and 50% of RAC, the slump value decreased to 80 mm, and 75 mm, respectively. This decrease in workability is due to the higher bulk density of RAC, which creates small pores in the cement matrix and occupies less volume in the concrete mix, making it more permeable and less flowable. The addition of macro-steel s hinders aggregate movement, reducing the workability of fresh concrete. The workability of RAC 50-SF 1-PP 0.5 concrete reduces from 80 mm to 68 mm with the addition of 1% macro-steel fiber. For HFRRAC, the workability drops even more to 76 mm and 72 mm when coarse aggregate is replaced by 25% and 0.75% macro-steel and 0.25% micro-PP are added, respectively. The accumulation of micro-PP fibers leads to the balling effect, which tends to reduce the workability of concrete.

Table 4. Slump and mechanical properties of RAC and HFRRAC

Specimen ID	Slump	Compressive Strength (N/mm^2)	Splitting Tensile Strength (N/mm^2)	Flexural Strength (N/mm^2)	Modulus of Elasticity (GPa)
Control Mix	83	30.2	2.12	4.3	27
RCA 25	80	31.33	1.98	4.1	27.56
RCA 50	78	34.23	2.55	4.45	27.9
RCA 25 – SF 0.5	77	33.78	3.11	4.75	28.2
RAC 25 – SF 0.75 – PP 0.25	76	21.56	2.83	3.45	27.92
RAC 25 – SF 1- PP 0.5	75	34.23	1.84	3.95	28.5
RAC 50 – SF 0.5	73	40.67	3.4	4.05	30
RAC 50 – SF 0.75 – PP 0.25	72	36.89	3.4	4.5	28.4
RAC 50 – SF 1 – PP 0.5	68	20.01	1.84	3.25	28.72
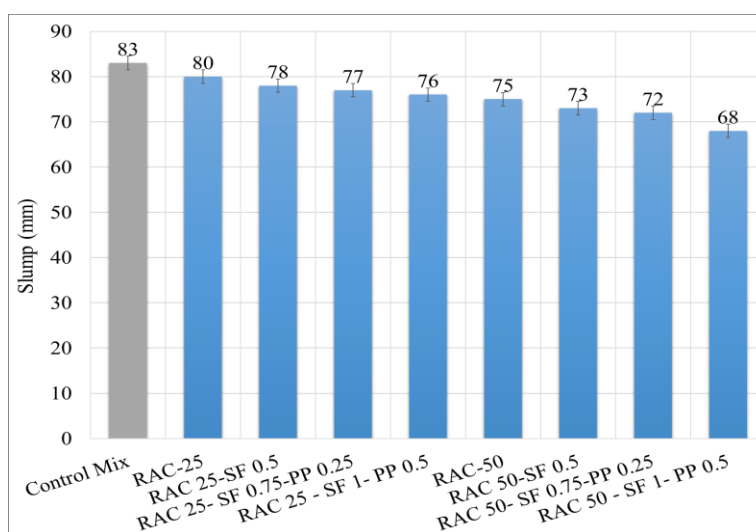
Figure 7. Variation of slump for control mix, RAC and HFRAC

3.2 Compressive strength of recycled aggregate concrete and hybrid fiber reinforced recycled aggregate concrete

The compression test was done on cubes of size 150mm x 150mm x 150mm specimens, which were dried in an oven after a curing period of 28 days. When compared to the control mix, the addition of 25% recycled aggregate leads to a minor increase in compressive strength (31.33 MPa). The addition of 0.5% macro-steel s increases the strength by 3 MPa in FRRAC specimens. In HYRAC, the addition of 0.5% PP s reduces the compressive strength to 21.56 MPa. An excess number of micro-fibers reduces the workability of concrete and increases the pores in the concrete specimen, which leads to a decrease in strength. While varying the composition of macro-steel s in concrete, it was noted that with an increase in the concentration of macro-steel s along with the addition of micro-PP fibers, the strength of the concrete decreased, and for the RAC 25-SF 1-PP 0.5 mix, a considerable drop in strength can be observed. However, the mix constituting RAC and steel fibers alone showed the maximum strength achieved after 28 days in the RAC 50 – SF 0.5 mix. Similarly, for a 50% replacement of aggregate with RAC, an increase in the SF composition alone resulted in an increase in strength for up to 0.5% SF. Beyond 0.5% SF, and the addition of micro-PP s slightly reduces the strength. The results conclude that the RAC 50-SF 0.5 mix is the most optimal mix for designing concrete that can withstand high compressive strength. Figure 8 illustrates the variation in compressive strength for the control mix, RAC,

and hybrid -reinforced concrete. Despite the addition of excess microfibers reducing the strength, Figure 9 shows a wide range of cracks spreading throughout the entire specimen in the cube failure pattern. The poor compaction of the concrete mix with microfibers may be the cause of the strength reduction. Therefore, the micro-s help to disperse the cracks and prevent sudden failure of the concrete specimen.

3.3 Flexural strength of recycled aggregate concrete and hybrid fiber reinforced recycled aggregate concrete

Table 4 provides the flexural strengths of the control specimens, RAC, FRRAC, and HFRRAC. The control specimen's flexural strength was 4.3 MPa, which decreased by 4% for a 25% aggregate replacement with RAC. Flexural strength, like compression and splitting tensile strength, increases with the addition of SF and hybrid . For hybrid fiber, RAC 25-SF 1-PP 0.5 showed reduced flexural strength (3.4 MPa) which is like the previous test results. When 0.75% macro-steel and 0.25% micro-PP were added to the control mix (CM), the strength of the hybrid -reinforced mix went up by 9.5%. The addition of increases the post-peak toughness of the beam under flexural load. All the s embedded in the concrete matrix contribute to stress transfer until the specimen fails, a process that occurs once the s reach their ultimate capacity. For a 50% replacement of RAC, the flexural strength values range from 3.95 MPa, 4.05 MPa, 4.5
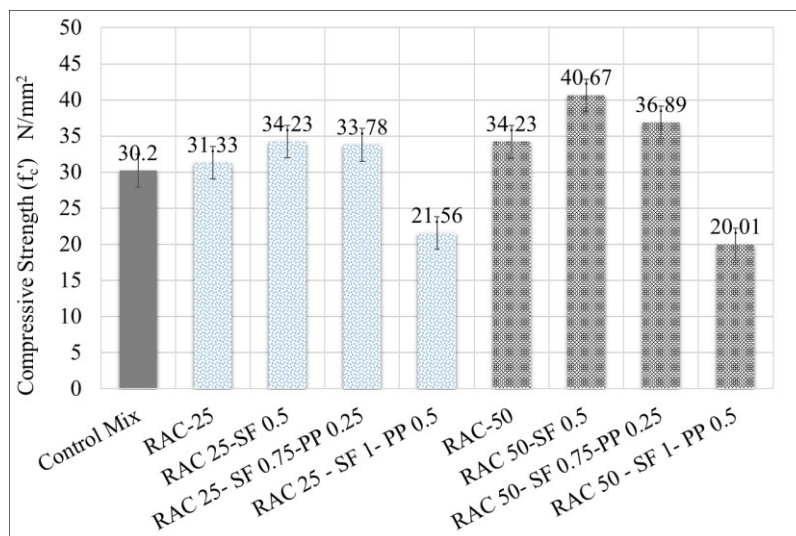
Figure 8. Compression strength of RAC and HFRRAC

Figure 9. Formation of micro cracks in hybrid fiber reinforced recycled aggregate concrete (a) 25% RAC & (b) 50% RAC
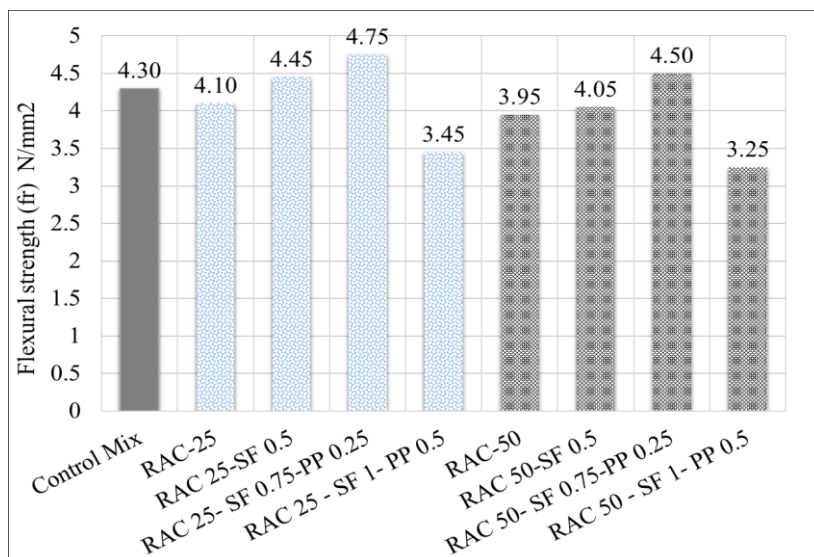
Figure 10. Flexural strength of RAC and HFRRAC
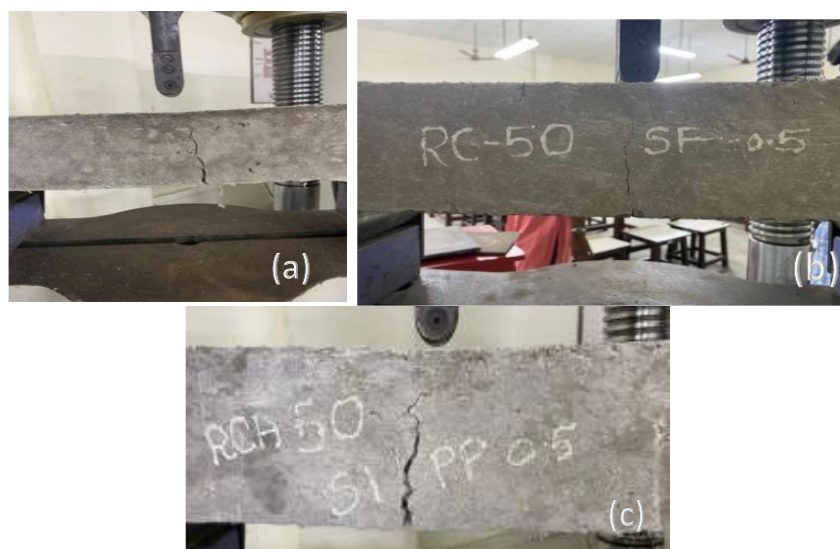
Figure 11 flexural test of (a) RAC (b) SFRAC, & (c) HFRRAC

MPa, and 3.25 MPa for RAC 50, RAC 50-SF 0.5, RAC 50-SF 0.75-PP 0.25, and RAC 50-SF 1-PP 0.5, respectively. Figure 10 illustrates the variation in flexural strength. The present flexural strength values agree well with the previous research findings. Figure 11 (a–c) displays the failure pattern for the control mix, FRRAC, and HFR RAC.for the control mix, FRRAC, and HFR RAC.

3.4 Modulus of elasticity of recycled aggregate concrete and hybrid fiber reinforced recycled aggregate concrete

Within the elastic region, the ratio of stress and corresponding strain measures the value of modulus of elasticity (MoE) of concrete. Since concrete is a brittle material, the addition of macro-steel s helps to improve the strength properties, mainly the compression, and flexural strength, thereby increasing the modulus of elasticity value. Figure 12 illustrates the variation in MoE between RAC and HFRRAC materials. For the control specimen, the MoE was 27 GPa, which slightly increased to 27.6 GPa with the

addition of 25% RAC. The orientation of the macro-steel fibers helps to increase the concrete mix's modulus of elasticity. The addition of SF and PP leads to an increase in the modulus of elasticity (MoE), which is in line with the values for compression, tension, and flexural strength. When we replace 50% of the aggregate with recycled aggregate and 0.5% SF, the modulus of elasticity (MoE) increases to 30 GPa (RAC 50–SSF 0.5), indicating a 10% increase compared to the control mix. For the fourth series of specimens, namely the RAC 25-SF 1-PP 0.5, the MoE decreases to 27.9 GPa.RAC 50, RAC 50- SF 0.5, RAC 50-SF 0.75 – PP 0.25 and RAC 50 – SF 1 – PP 0.5 the MoE values were 28.5 GPa, 30 GPa, 28.4 GPa, and 28.7 GPa, respectively. The voids in the concrete mix decrease with the amount of SF and PP, which also increase the strength of the concrete and thereby the MoE value. Therefore, we can conclude that the addition of RAC, SF, and PP s reduces the strain in the concrete under the applied compression load, thereby increasing the modulus of elasticity. Figure 13 displays the specimen that failed the axial compression test.
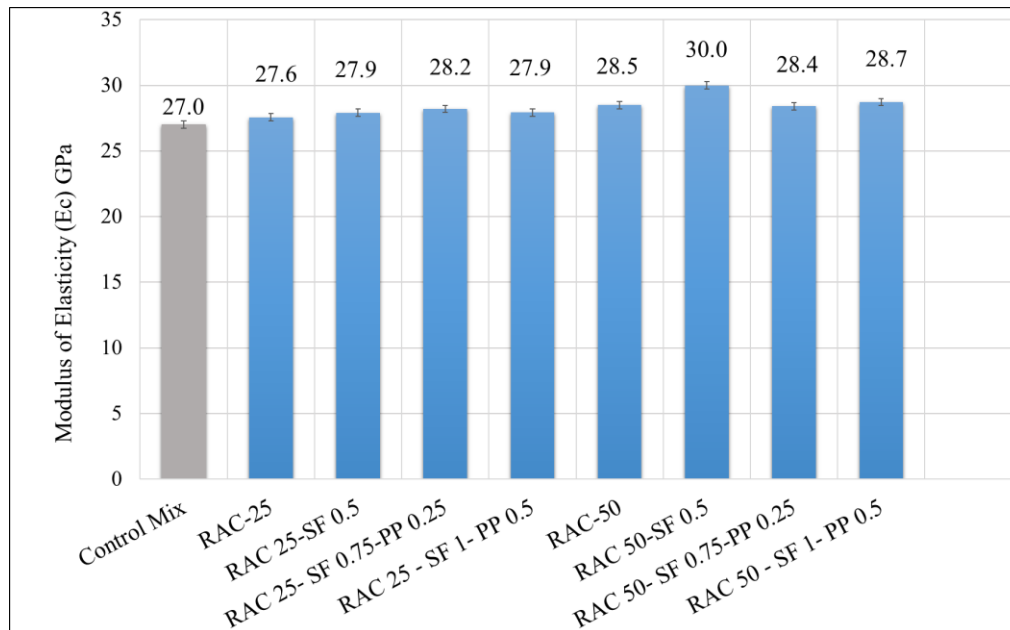
Figure 12. Modulus of elasticity of RAC, SFRAC and HFRRAC specimens

Figure 13. Tested specimen for Modulus of elasticity

.

3.5 Water absorption of recycled aggregate concrete and hybrid fiber reinforced recycled aggregate concrete.

For the water absorption test, the specimens were dried in an oven for a specified time and temperature and then placed in a desiccator to cool. Immediately upon cooling, the dry weight of the specimen was recorded. The cylinder specimen was then partially immersed in water to allow capillary movement of water particles through the specimen. The weight of the specimen was measured at regular intervals until the saturation condition was reached. For the normal mix, the dry weight of the specimen was found to be 0.88 kg, and the weight after 30 minutes and 3 days was found to be 0.89 kg, and 0.91 kg, respectively, with an initial water absorption of 1.14% and a final water absorption of 3.41%. Increasing the amount of recycled aggregate in concrete leads to an increase in water absorption. The water absorption percentages after 30 minutes were 1.83%, and

1.82% for RAC 20, and RAC 50, respectively. For macro-steel -reinforced RAC, the water absorption percentage was 1.54% and 2.06% for RAC 25-05 SF. With the addition of hybrid s, the water absorption percentage increased with the increase in micro-PP content. We observed the highest water absorption value for RAC 25-1 SF + 0.55 PP, with an initial water absorption of 8.57% and a final absorption of 16.29%. An increase in the weight of the specimen after immersing it in water reflects that with the increase in RAC composition, the water absorption increases, which is due to the presence of old concrete particles adhering to the aggregate. Also, the PP s tend to increase the water absorption percentage, which is mainly due to the increase in porosity of the concrete specimen. Table 5 tabulates the water absorption test results. Figure 14 displays the initial water absorption and final after-absorption of RAC, SFRAC, and HFRRAC.

Table 5. Water absorption test result

Specimen ID	Dry weight of Specimen (kg)	Weight of specimen after 30 min (kg)	Weight of specimen after 3 days (kg)	Initial Water Absorption (30 min) %	Final water Absorption % (After 3 days)
Control mix	0.88	0.89	0.91	1.14	3.41
RCA-25	0.872	0.888	0.919	1.83	5.39
RCA-50	0.879	0.895	0.926	1.82	5.35
RCA-25-0.5SF	0.91	0.924	0.957	1.54	5.16
RCA-50-0.5SF	0.923	0.942	0.974	2.06	5.53
RAC-25-0.75SF-0.25PP	0.852	0.872	0.91	2.35	6.81
RAC-50-0.75SF-0.25PP	0.868	0.888	0.931	2.30	7.26
RAC-25-1SF-0.5PP	0.669	0.733	0.778	9.57	16.29
RAC-50-1SF-0.5PP	0.665	0.722	0.778	8.57	16.99
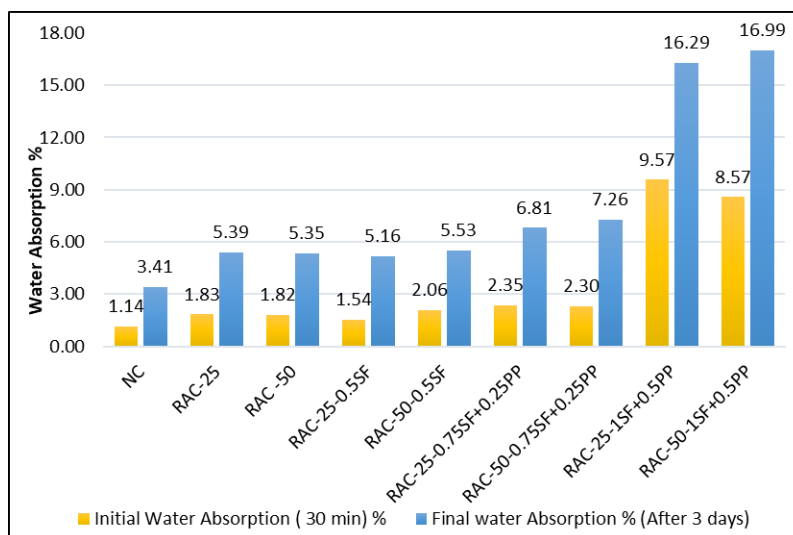
Figure 14. Water absorption percentages after 30 minutes and 3 hours RAC and HFRRAC specimens

3.6 Acid attack test

Acid resistance refers to a material or colour's ability to resist degradation upon exposure to acid. Durability tests of acid resistance of concrete were determined in terms of weight loss and residual compressive strength. We cast and cure concrete cubes for this test, noting their initial dry weight before conducting the acid resistance test. Next, we immerse the cubes in sulfuric acid for three days, remove them, give them a thorough rub, and note their weight after three days. The cubes are again immersed in the sulphuric acid for seven days. The weight of the cubes after seven days of acid attack is noted. The cubes are cleaned, rubbed, and again immersed in acid for 14 days, the weight of the cubes is noted. The comparative weight of the cubes after immersing in acid is noted on the third, the seventh and the fourteenth day to check the durability of the cubes. Table 6 tabulates the amount of weight loss in the concrete specimen following acid exposure. Compared to the control mix, the percentage weight loss for RAC was 3.42% and 7.57% for RAC 25 and RAC 50, respectively. With the addition of s, the weight loss

due to acid attack increased slightly to 4.97 and 7.27 for RCA-25-0.5SF and RCA-50-0.5SF respectively. For hybrid - reinforced concrete, the weight was observed to be a maximum of 10.92% for RAC-50-1SF-0.5PP. Thus, the addition of s tends to slightly increase the pores in concrete and thereby increase the possibility of acid attack.

Figure 15 shows the surface of the specimen exposing the s after 7 and 14 days in an acid environment. After 14 days, the compressive strength of the cube specimen subjected to an acid environment was tested and tabulated in Table 7. Figure 16 shows the variation of strength after acid attack. The results showed that the macro-steel - reinforced specimen's strength was approximately 20 Mpa and 15 Mpa for 25% and 50% RAC replacement, respectively. For hybrid reinforcement, the strength was 24 MPa and 22 Mpa which is slightly lower when compared to control specimen. Thus, the addition of s tends to improve the strength properties of concrete both, in a normal as well as an acidic environment. But an increase in the micro content reduces the strength due to an increase in the porosity of the concrete specimen.

Table 6. Specimen weight loss after acid attack

Specimen	Dry weight of the cube (kg)	3rd day weight of the cube (kg)	7th day weight of the cube (kg)	14th day weight of the cube (kg)	Percentage weight loss after 14 days (%)
Control mix	2.484	2.46	2.43	2.40	3.38
RCA-25	2.340	2.32	2.30	2.26	3.42
RCA-50	2.337	2.31	2.25	2.16	7.57
RCA-25-0.5SF	2.336	2.30	2.26	2.22	4.97
RCA-50-0.5SF	2.448	2.41	2.36	2.27	7.27
RAC-25-0.75SF-0.25PP	2.450	2.42	2.39	2.35	4.08
RAC-50-0.75SF-0.25PP	2.563	2.53	2.47	2.35	8.31
RAC-25-1SF-0.5PP	2.287	2.263	2.20	2.17	5.12
RAC-50-1SF-0.5PP	2.391	2.37	2.26	2.13	10.92

Figure 15. Acid attack specimen after (a) 7 days and (b) 14 days

Table 7. Acid attack test compressive strength

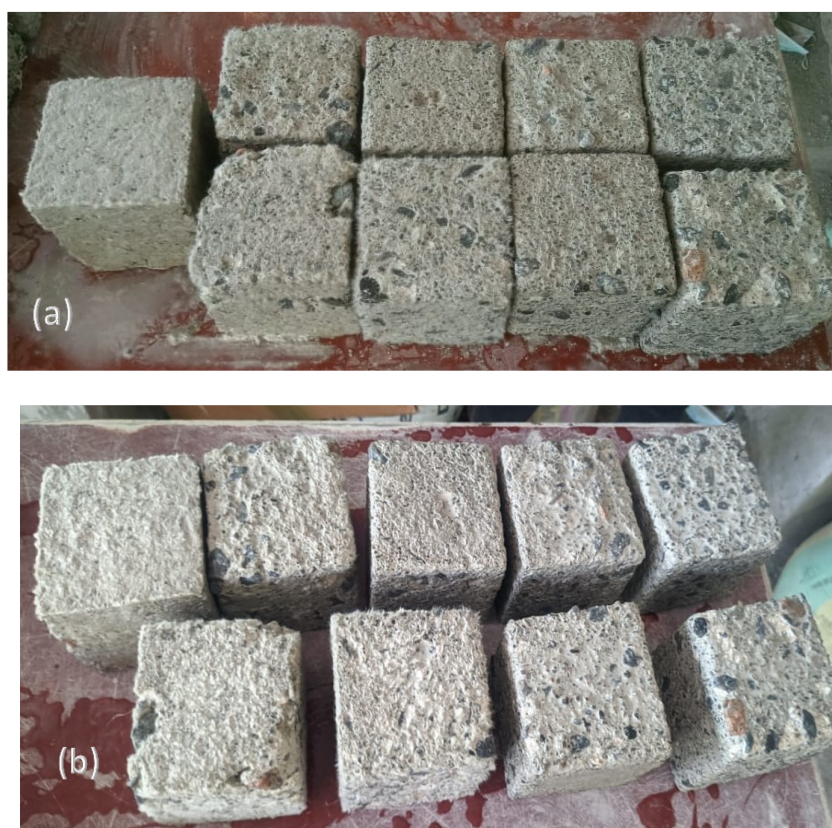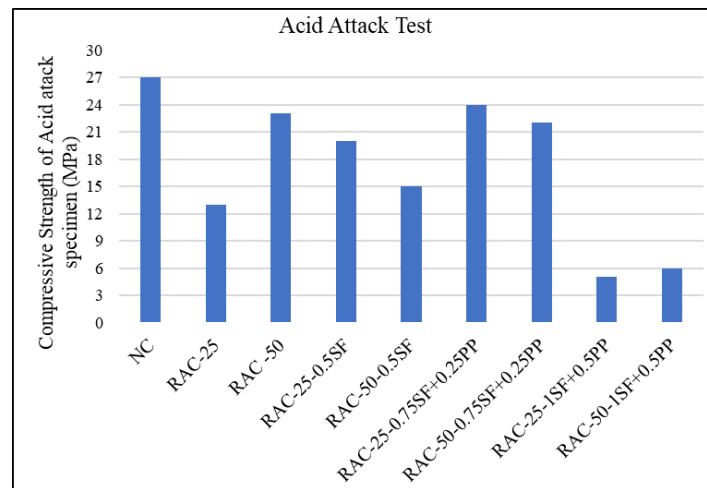| Specimen ID	Compressive strength (N/mm^2)
NC	27
RAC-25	13
RAC -50	23
RAC-25-0.5SF	20
RAC-50-0.5SF	15
RAC-25-0.75SF+0.25PP	24
RAC-50-0.75SF+0.25PP	22
RAC-25-1SF+0.5PP	5
RAC-50-1SF+0.5PP	6

Figure 16. Compressive strength of RAC & HFRRAC specimen subjected to acid environment.

4 Conclusion

From the experimental investigation carried out to study the mechanical and durability properties of RAC and HFRRAC, the following conclusions can be derived:

- The control mix recorded a slump of 83 mm, which decreased as the percentage of RAC, SF, and PP increased. For the mixes RAC 25, RAC 25-SF 0.5, RAC 25-SF 0.25- PP 0.25, RAC 25- SF 1- PP 0.5, RAC 50, RAC 50- SF 0.5, RAC 50- SF 0.75 – PP 0.25 and RAC 50 – SF 1 – PP 0.5 the slump value decreases to 80mm, 78mm, 77mm, 76mm, 76mm, 75mm, 73mm, 72mm, 68mm.
- The RAC mix's compressive strength increased by up to 4% compared to the unreinforced mix (CM). The compressive strength of the HFRRAC increases and then decreases as the percentage of macro steel increases.
- The addition of RAC, SF, and PP s increases and decreases the flexural strength. For HFRRAC, the strength properties decrease as the percentage of macro-SF increases. The reduction in strength properties with the increase in the percentage of macro-SF is due to the orientation of SF fibers, bond between the aggregate and cement matrix.
- The modulus of elasticity value increases with the addition of RAC, macro-SF and micro-PP s. For HFRRAC, the strength properties increase as the percentage of macro-SF and micro-PP increases. The orientation of the aggregate, the bond between the aggregate and cement matrix, or the elongated shape of the aggregate all contribute to the increase in strength properties as the percentage of coconut shell increases.
- None of the tested specimens showed evidence of fracture in the recycled aggregate, demonstrating its unrestricted use as a replacement for conventional aggregate. Therefore, it can be concluded that RAC, macro-steel and micro-polypropylene can be effectively used as reinforcement in concrete to produce a sustainable concrete solution.

Declarations:

CRediT authorship contribution statement:
Vijayalakshmi. R: Investigation and Writing – original draft
Javith Shainsha: Investigation and data curation
Madhuru Harshitha: Investigation and data curation
Oshiyana Ramadoss: Investigation and data curation

Acknowledgements

References

[1] K. I. R. Akça, Ö. Çakir, and M. Ipek, "Properties of polypropylene fiber reinforced concrete using recycled aggregates," *Constr. Build. Mater.*, vol. 98, pp. 620–630, 2015, doi: 10.1016/j.conbuildmat.2015.08.133.

[2] G. M. Chen, H. Yang, C. J. Lin, J. F. Chen, Y. H. He, and H. Z. Zhang, "Fracture behaviour of steel reinforced recycled aggregate concrete after exposure to elevated temperatures," *Constr. Build. Mater.*, vol. 128, pp. 272–286, 2016, doi: 10.1016/j.conbuildmat.2016.10.072.

[3] Q. Zhang, X. Feng, X. Chen, and K. Lu, "Mix design for recycled aggregate pervious concrete based on response surface methodology," *Constr. Build. Mater.*, vol. 259, 2020, doi: 10.1016/j.conbuildmat.2020.119776.

[4] J. A. Carneiro, P. R. L. Lima, M. B. Leite, and R. D. Toledo Filho, "Compressive stress-strain of steel fiber reinforced-recycled aggregate concrete," *Cem. Concr. Compos.*, vol. 46, pp. 65–72, 2014, doi: 10.1016/j.cemconcomp.2013.11.006.

[5] M. A. Al-Osta, A. S. Al-Tamimi, S. M. Al-Tarbi, O. S. Baghabra Al-Amoudi, W. A. Al-Awsh, and T. A. Saleh, "Development of sustainable concrete using recycled high-density polyethylene and crumb tires: Mechanical and thermal properties," *J. Build. Eng.*, vol. 45, no. September 2021, p. 103399, 2022, doi: 10.1016/j.jobe.2021.103399.

[6] K. Cui *et al.*, "Mechanical of multiscale hybrid fiber reinforced recycled aggregate concrete subject to uniaxial compression," *J. Build. Eng.*, vol. 71, no. April, p. 106504, 2023, doi: 10.1016/j.jobe.2023.106504.

[7] S. Abdallah, D. W. A. Rees, S. H. Ghaffar, and M. Fan, "Understanding the effects of hooked-end steel geometry on the uniaxial tensile behaviour of self-compacting concrete," *Constr. Build. Mater.*, vol. 178, pp. 484–494, 2018, doi: 10.1016/j.conbuildmat.2018.05.191.

[8] A. Toghroli, P. Mehrabi, M. Shariati, N. T. Trung, S. Jahandari, and H. Rasekh, "Evaluating the use of recycled concrete aggregate and pozzolanic additives in fiber-reinforced pervious concrete with industrial and recycled fibers," *Constr. Build. Mater.*, vol. 252, p. 118997, 2020, doi: 10.1016/j.conbuildmat.2020.118997.

[9] D. V. Soulioti, N. M. Barkoula, A. Paipetis, and T. E. Matikas, "Effects of geometry and volume fraction on the flexural behaviour of steel- reinforced concrete," *Strain*, vol. 47, no. SUPPL. 1, pp. 535–541, 2011, doi: 10.1111/j.1475-1305.2009.00652.x.

[10] A. A. Elakhras, M. H. Seleem, and H. E. M. Sallam, "Intrinsic fracture toughness of fiber reinforced and functionally graded concretes: An innovative approach," *Eng. Fract. Mech.*, vol. 258, no. November, p. 108098, 2021, doi: 10.1016/j.engfracmech.2021.108098.

[11] S. Guler, B. Öker, and Z. F. Akbulut, "Workability, strength and toughness properties of different types of fiber-reinforced wet-mix shotcrete," *Structures*, vol. 31, no. January, pp. 781–791, 2021, doi: 10.1016/j.istruc.2021.02.031.

[12] A. Bhutta, P. H. R. Borges, C. Zanotti, M. Farooq, and N. Banthia, "Flexural of geopolymer composites reinforced with steel and polypropylene macro fibers," *Cem. Concr. Compos.*, vol. 80, pp. 31–40, 2017, doi: 10.1016/j.cemconcomp.2016.11.014.

[13] B. H. AbdelAleem and A. A. A. Hassan, "Influence of synthetic fibers' type, length, and volume on enhancing the structural performance of rubberized concrete," *Constr. Build. Mater.*, vol. 229, p. 116861, 2019, doi: 10.1016/j.conbuildmat.2019.116861.

[14] T. Simões, H. Costa, D. Dias-da-Costa, and E. Júlio, "Influence of type and dosage of micro-s on the physical properties of reinforced mortar matrixes," *Constr. Build. Mater.*, vol. 187, pp. 1277–1285, 2018, doi: 10.1016/j.conbuildmat.2018.08.058.

[15] C. Unterweger *et al.*, "Impact of fiber length and fiber content on the mechanical properties and electrical conductivity of short carbon fiber reinforced polypropylene composites," *Compos. Sci. Technol.*, vol. 188, no. January, p. 107998, 2020, doi: 10.1016/j.compscitech.2020.107998.

[16] A. Zia and M. Ali, " of fiber reinforced concrete for controlling the rate of cracking in canal-lining," *Constr. Build. Mater.*, vol. 155, pp. 726–739, 2017, doi: 10.1016/j.conbuildmat.2017.08.078.

[17] M. Pajak, "Investigation On Flexural Properties of Hybrid Reinforced Self-Compacting Concrete," vol. 161, pp. 121–126, 2016, doi: 10.1016/j.proeng.2016.08.508.

[18] A. Elbehiry, O. Elnawawy, M. Kassem, A. Zaher, and M. Mostafa, "FEM evaluation of reinforced concrete beams by hybrid and banana fiber bars (BFB)," *Case Stud. Constr. Mater.*, vol. 14, p. e00479, 2021, doi: 10.1016/j.cscm.2020.e00479.

[19] E. Yooprasertchai, P. Wiwatrojanagul, and A. Pimanmas, "A use of natural sisal and jute fiber composites for seismic retrofitting of nonductile rectangular reinforced concrete columns," *J. Build. Eng.*, vol. 52, no. April, p. 104521, 2022, doi: 10.1016/j.jobe.2022.104521.

[20] V. Ramalingam, "Study on the performance of GFRP strengthened, fiber reinforced lightweight foam concrete," *Gradjevinski Mater. i Konstr.*, vol. 65, no. 4, pp. 137–148, 2022, doi: 10.5937/grmk2204137r.

[21] R. Sathia and R. Vijayalakshmi, "Fresh and mechanical property of caryota-urens fiber reinforced flowable concrete," *J. Mater. Res. Technol.*, vol. 15, pp. 3647–3662, 2021, doi: 10.1016/j.jmrt.2021.09.126.

[22] O. Gencel *et al.*, "Basalt fiber-reinforced foam concrete containing silica fume: An experimental study," *Constr. Build. Mater.*, vol. 326, no. February, p. 126861, 2022, doi: 10.1016/j.conbuildmat.2022.126861.

[23] A. I. Al-hadithi, A. Tareq, and W. Khairi, "Mechanical properties and impact of PET fi ber reinforced self-compacting concrete (SCC)," *Compos. Struct.*, vol. 224, no. July 2018, p. 111021, 2019, doi: 10.1016/j.compstruct.2019.111021.

[24] S. Ramalingam, V. Ramalingam, R. Srinivasan, V. Gopinath, Y. Ramanareddy, and Y. Ramanareddy, "Uni Axial Compression Behaviour of Lightweight Expanded Clay Aggregate Concrete Cylinders Confined by Perforated Steel Tube and Gfrp Wrapping," *Rev. la Constr.*, vol. 19, no. 3, pp. 200–212, 2020, doi: 10.7764/RDLC.19.3.200.

[25] T. F. Yuan, J. Y. Lee, K. H. Min, and Y. S. Yoon, "Experimental investigation on mechanical properties of hybrid steel and polyethylene fiber-reinforced no-slump high-strength concrete," *Int. J. Polym. Sci.*, vol. 2019, 2019, doi: 10.1155/2019/4737384.

[26] K. Turk, M. Bassurucu, and R. Enes, "Workability , strength and flexural toughness properties of hybrid steel fiber reinforced SCC with high-volume fiber," *Constr. Build. Mater.*, vol. 266, p. 120944, 2021, doi: 10.1016/j.conbuildmat.2020.120944.

[27] B. Raj, D. Sathyan, M. K. Madhavan, and A. Raj, "Mechanical and durability properties of hybrid fiber reinforced foam concrete," *Constr. Build. Mater.*, vol. 245, p. 118373, 2020, doi: 10.1016/j.conbuildmat.2020.118373.

[28] J. Liu, H. Jin, X. Zhao, and C. Wang, "Effect of multi-walled carbon nanotubes on improving the toughness of reactive powder concrete," *Materials (Basel).*, vol. 12, no. 16, 2019, doi: 10.3390/ma12162625.

[29] R. Bajaj, B. Wang, and R. Gupta, "Characterization of enhanced itz in engineered polypropylene fibers for bond improvement," *J. Compos. Sci.*, vol. 4, no. 2, 2020, doi: 10.3390/jcs4020053.

Technical paper

Enhancing RCF rail defect inspection on the Serbian railway network

Zdenka Popović[1)], Ljiljana Brajović[1)], Milica Mićić[1)], Luka Lazarević[*1)]

[8)] Faculty of Civil Engineering, University of Belgrade, Bulevar kralja Aleksandra 73, 11120 Belgrade, Serbia

A B S T R A C T

The interaction between the wheel and the running rails within the railway system introduces intricate stress patterns, resulting in the formation of rolling contact fatigue (RCF) rail defects. The magnitude of this stress is contingent upon factors such as track performance, vehicle characteristics, and service conditions. While advancements in rail metallurgy can mitigate the issue to some extent, no economically viable steel composition currently exists that can completely withstand the repetitive stresses associated with RCF. It is more cost-effective to properly maintain rails for longer use rather than replace them entirely. The paper emphasizes the importance of classifying and coding RCF rail defects in light of their potential adverse effects on rail transport safety. It provides an analysis of the available inspection methods for RCF rail defects and recommends the ones that should be implemented on the Serbian railway network. A combination of proposed inspection methods is preferred to increase detection efficiency for different types of RCF defects.

1 Introduction

The Serbian railway network is a crucial link connecting Southeast Europe to the broader European railway network. Serbia, as an essential transportation corridor, plays a crucial role in facilitating efficient connections between Eastern and Western Europe. Its strategic geographical location makes it a pivotal trade hub, allowing for the efficient transportation of goods and passengers. Improvements and modernization of the railway infrastructure in Serbia directly impact the overall efficiency of the European transportation system [1]. This, in turn, fosters economic cooperation, trade, and mobility within Europe. Therefore, investments in the Serbian railway network not only contribute to the country's regional development but also strengthen its integration into the European transportation system.

The railway density in Serbia is 49.2 km/1000km^2, similar to the EU average of 50.1 km/1000km^2. The Serbian railway network spans 3819 km.The crucial part of this network is the European Corridor X (Figure 1), which has two branches leading towards Hungary (Belgrade-Budapest) and Bulgaria (Niš-Sofia). Corridor X is an important part of the southeastern multimodal axis, which connects the following countries: Austria/Hungary, Slovenia/Croatia, Serbia, and Bulgaria/North Macedonia/Greece. The modernization and reconstruction of the railway infrastructure on Corridor X through Serbia aim to increase train speeds to 200 km/h and axle loads to 225 kN.

An increase in vehicle speed, traffic density, and axle loads on the railway lines in Serbia could lead to the significant appearance and development of rail defects caused by rolling contact fatigue (RCF), which adversely affects maintenance costs, noise, and vibration emissions and could endanger traffic safety. RCF implies rail damage caused by the complex stresses that are characteristic of rail-wheel rolling contact (Figure 2). To ensure safe railway transport, efficient inspection methods are crucial in detecting RCF rail defects.

In their previous paper [2], the authors presented and described representative types of non-destructive inspection methods, both conventional and innovative, with a focus on their basic characteristics, advantages, and disadvantages. The research [2] was based on numerous international research studies and representative published papers. The purpose of the research [2] was to identify practical applications for inspection methods in the railway industry and suggest ways to enhance equipment and software for better results in rail inspection. The authors recommended combining multiple inspection methods to improve rail defect detection performance [2].

In this paper, the authors focus on improving the RCF rail defect inspection procedure by using modern, non-destructive methods to detect these defects on the railway network in Serbia. The goal is to efficiently detect RCF defects on in-service running rails using manual or installed equipment on commercial or inspection vehicles. The effective inspection of RCF rail defects should be the basis for reactive, scheduled, and predictive maintenance of rails in service.

---

[*] Corresponding author:
E-mail address: llazarevic@grf.bg.ac.rs
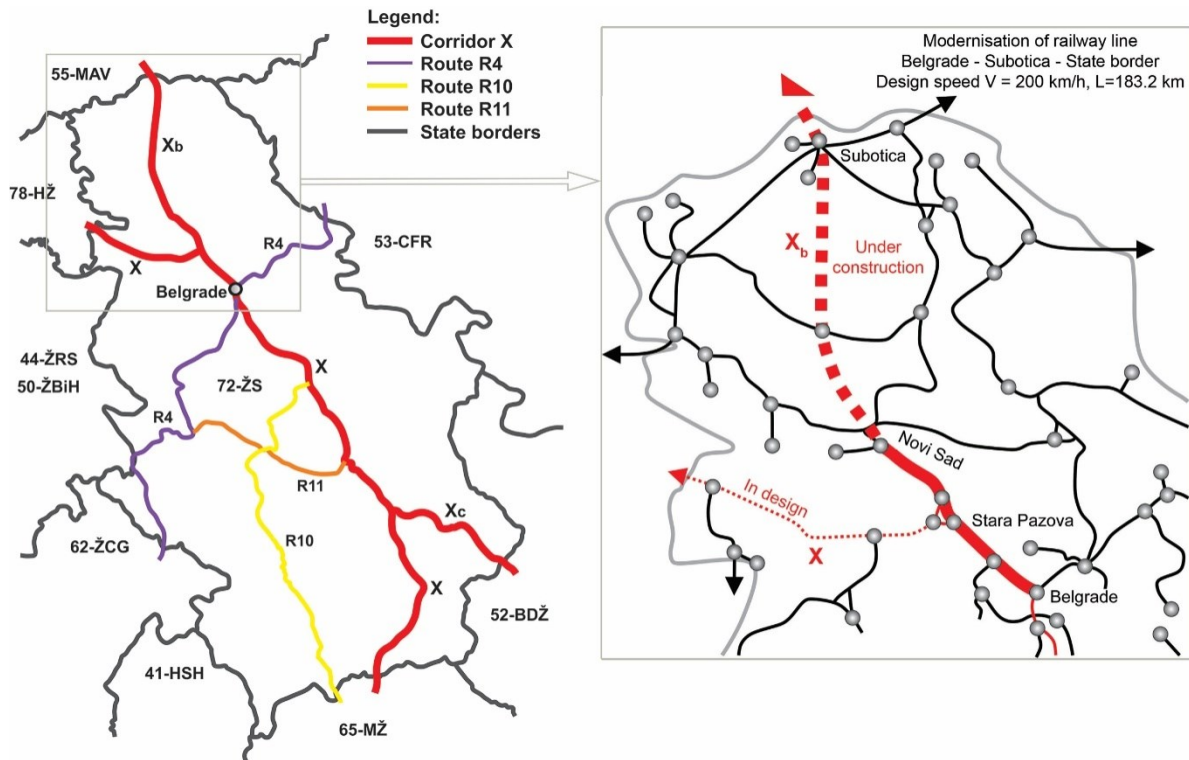
Figure 1. Main railway lines through the Republic of Serbia (left) and modernised railway line for speeds up to 200 km/h (right)
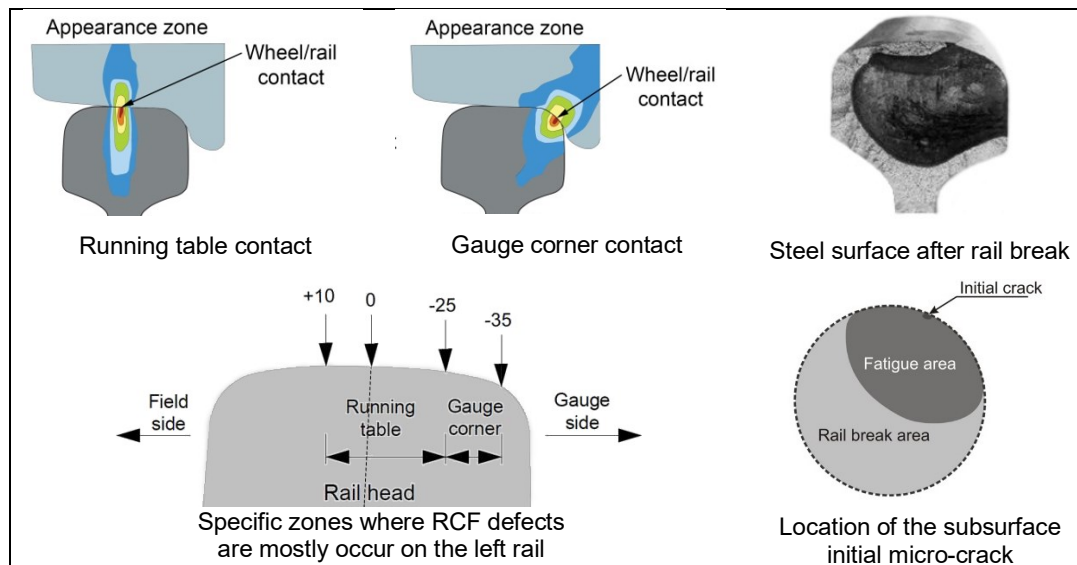
Figure 2. Contact zones with complex RCF stress on the left running rail

2 Brief review of RCF rail defects and coding system

In 2018, the general classification and coding system for the RCF rail defects caused by the complex stresses that are characteristic of rail/wheel contact were provided by IRS 70712 [3] and EN 16729-3 [4]. Furthermore, EN 13231-5 [5] provides defect definitions without a coding system. The paper [6] deals with the incompatibility of European standards [4,5] with UIC recommendations [3, 7, 8], which could create difficulties and misunderstandings in applying coding system (Table 1).

RCF defects can be extremely dangerous for railway traffic, causing harm to both human lives and the environment. They can result in injuries, material damage, and other catastrophic incidents [9, 10]. Therefore, it is essential to have an accurate coding system to track the occurrence of such defects. A uniform coding system used throughout the EU network would be beneficial for statistical analysis purposes and help identify the areas that require immediate attention to prevent any further damage.The Infrastructure Manager (IM) has to define a Rule book with the following data about a rail defect to achieve successful inspection and maintenance of rail defects:

− the official name of the rail defect in both Serbian and English,

− a standard benchmark photo indicating the characteristic appearance and location of the defect on the rail

− a brief description, including data on the location and cause of the occurrence,

− recommended methods for detection,

− recommendations for condition monitoring and maintenance,

− a unique numerical code, and

− necessary comments indicating the degree of danger it poses to railway transport safety.

Table 1. Inconsistencies in the RCF rail defect coding system

Benchmark photo	Brief definition by EN 13231-5	Numbering codes and comments
	Head checking (HC) Small parallel cracks on the rail head near the gauge corner.	− 1223, 2223 by IRS 70712 − 2223 by EN 16729-3, UIC Code 712 and UIC CODE 725
	Belgrospi A network of cracks developing on the rail head of track with a speed greater than 160 km/h affected by short-pitch corrugation.	− 2271 by EN 16729-3 − Not consider by IRS 70712
	Squat Rolling contact fatigue defect whose main characteristics are a blackish patch on the rail head, a lateral flow of steel and a collapsed and widened rolling band.	− 127, 227, 417, 427 by IRS 70712 and EN 16729-3 − 2271,437 by IRS 70712
	Flaking Surface condition consisting of the gouging of metal on the railhead.	− 2222 Shelling of the gauge corner by UIC Code 712, − 1221, 2221 by IRS 70712
	Spalling Cracking and chipping on the top of the rail.	− 1211, 2211 by IRS 70712
	Side cutting Wear occurring on high rails in small radius curves where wheel flanges contact the rail.	− 2203 by IRS 70712

	Lipping	Not consider by IRS 70712
	Lipping Plastic metal flow occurring on the rail head under conditions of high axle load and high gross tonnage.	The lippingdefect is a manifestation of HC defect on a track with variable traffic direction (e.g. single track line).
	Short pitch corrugation Quasi-periodic irregularities on the running surface. The wavelength usually is 10 mm to 100 mm. The short-pitch corrugation is typically encountered in the straight track on both rails and large radius curves on the high rail.	2201 Code by IRS 70712 and definition as follows: Short-pitch corrugation is characterised by a pseudo-periodical sequence of bright ridges and dark hollows on the running surface with a pitch generally less than 8 cm. This defect can appear at any location. 2202 Code by IRS 70712 and definition as follows: Long-pitch corrugation is characterised by depressions in the running surface of the railhead of lower rail in curves and tangential tracks. The pitch varies between 8 and 30 cm. The progression of the corrugation depends on curve radius, cant deficiency/excess, steel grade, friction in wheel/rail contact, and vehicle characteristics. Short-wave corrugation and long-wave corrugation are not included in IRS 70712.
	Short wave corrugation Depressions in the running surface which are pronounced. The wavelength usually is 30 mm to 300 mm.	
	Long wave corrugation Irregular unevenness on the running surface. The wavelength usually is 300 mm to 1000 mm.	
	Wheel burn Abrasive, plastic and thermal damage occurring in zones where trains start to move.	– 2251, 2251 by IRS 70712 – 125, 2251, 2252, 445 by EN 16729-3

To prevent misunderstanding, the names *head checking*, *squat*, and *belgrospi* are used universally in scientific and professional documents without translation, due to the proven danger of causing multiple rail breaks under the vehicle. A significant number of research papers worldwide [11-19] deal with HC and squat rail defects due to their threat to railway safety.

In addition, corrugation is the topic of many scientific and professional papers. It has a direct impact on railway traffic comfort and initiates the deterioration of the railway infrastructure. Alternative forms of fatigue deterioration may arise due to the continuous interaction of the wheel with corrugation peaks, giving rise to a distinctive form of structural impairment referred to as "belgrospi". These rail defects manifest as cracks forming on the wave peaks and if left untreated, progress into more severe anomalies known as squats. This entails the emergence of a network of cracks on the corrugation crests, which resemble a combination of irregular headchecks and minor squats. The rail defect is named Belgrospi after being initially observed by German engineers Belz, Grohmann, and Spiegel on a German high-speed line. Belgrospi cracks pose a risk of consequential and substantial damage to rails. Research by Schoech [20] indicates that short-pitch corrugation with a depth of 0.03 mm can significantly elevate dynamic forces, leading to the development of such structural defects.

A visual inspection of the rails on the double-track railway Belgrade - Novi Sad for speeds up to 200 km/h, which was put into regular traffic on March 20, 2022, indicates the presence of RCF rail defects. On this railway line, belgrospi

rail defects were observed for the first time in Serbia. Figure 3 shows the development of corrugation and belgrospi defects on the corrugation crests. Figure 4 shows the development of a squat defect in a typical place next to a concrete sleeper due to a change in the vertical stiffness of the switch support. Figures 3 and 4 show the RCF rail defects in the railway section where preventive grinding of new rails was not carried out.

Figure 3. Belgrospi cracks forming on the corrugation peaks in the switch on the Stara Pazova – Novi Sad railway line (Photoby Aleksandar Milutinović in December 2023)

Figure 4. A squat defect developed right next to the concrete sleeper (Photo by Aleksandar Milutinović in Indjija station, December 2023)

It is essential to develop a plan for managing the emergence and progression of RCF defects on railways in Serbia. The first step is to develop regulations for classifying and coding rail defects, as well as mandatory training for professional staff. Following this, non-destructive methods should be chosen for early detection and monitoring of the development of rail defects. Lastly, the rails have to be repaired or removed.

3 Recommended NDT methods for RCF inspection of rail defects on the serbian railway network

The inspection methods for rail defects during the development of railway infrastructure and vehicles undergo cycles of progress and inactivity. Progress is driven by advancements in measurement devices, equipment, acquisition systems, and software for processing and analyzing recorded data (Figure 5). The effectiveness of these processes relies on the knowledge, economic, and management capabilities of the inspection management, as well as the skills of the employees who perform the inspection tasks.

Internal and external factors influencing each railway company's decision on choosing NDT (Non-Destructive Testing) methods for inspecting RCF rail defects can be diverse. Table 2 shows several factors that may impact the decision.
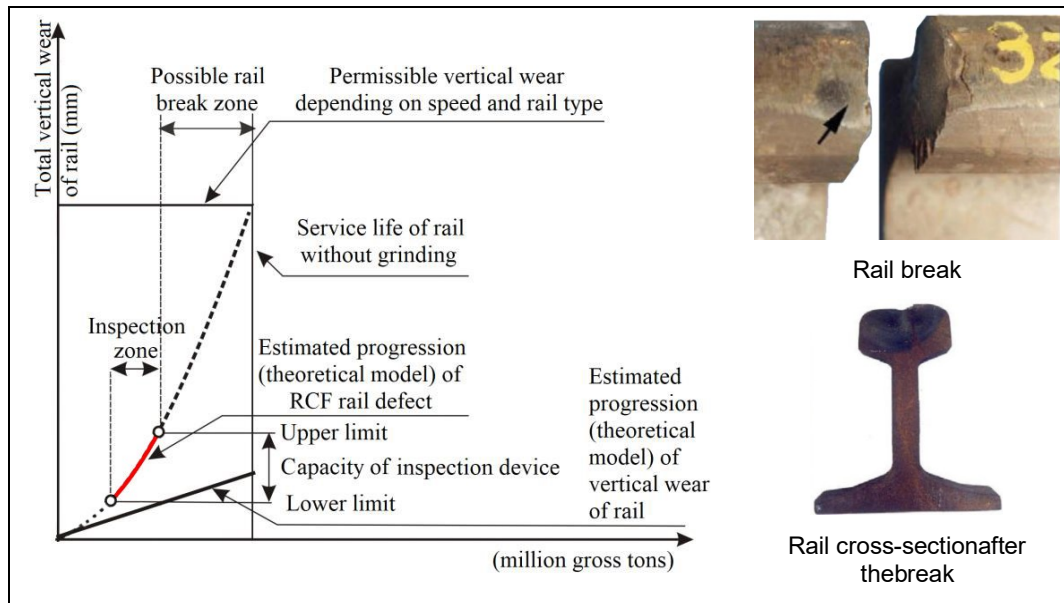
Figure 5. The capacity of inspection devices and their impact on the lifespan of the railway

Table 2. Overall factors influencing a railway company's decision on choosing NDT for inspecting RCF rail defects

Internal factors influencing a railway company's decision	
Financial Resources	The availability of financial resources for implementing a specific NDT method can be a crucial factor. Equipment costs, staff training, and maintenance expenses may limit the options.
Staff Expertise	For a particular NDT method to be successful, staff must be trained in its application. An internal factor includes having experts within the railway company familiar with a specific method.
Resource Availability	Depending on the company's size and capabilities, certain NDT methods may not be practical or feasible. In some cases, implementing specific NDT methods may not be practical or achievable due to limitations in the company's resources or infrastructure.
System Sustainability	Infrastructure and vehicle maintenance, as well as access to accurate system condition data, play a crucial role in selecting an appropriate NDT method.
External factors influencing a railway company's decision	
Regulations	Legal requirements and technical regulations may demand the use of specific NDT methods to ensure safety and compliance with Directives, TSIs, and EN standards.
Technological Advancement	Rapid technological developments in NDT can offer new and more efficient methods that the company may consider to enhance its inspection procedures.
Industry Developments	Changes in the railway transportation industry, such as new types of vehicles or increased speeds, can influence the need for more advanced inspection methods.
Social Responsibility	Increased awareness of environmental protection and accident reduction can affect the decision to use more precise inspection methods to minimise the risk of accidents.

All these factors together can influence the decision-making process regarding the selection of a suitable NDT method for inspecting RCF rail defects. The railway company needs to consider these factors to achieve a balance between efficiency, economic feasibility, and compliance with standards and regulations. Traditionally, Serbian railways use visual and ultrasonic methods to detect rail defects.

Figure 6 shows the different groups of methods available for detecting rail defects along with the methods that IM plans to apply (highlighted in grey in Figure 6). IM will achieve this by purchasing equipment and installing it on inspection or commercial vehicles. It is possible and sometimes preferable to use a combination of multiple testing methods.

Figure 7 shows in detail the specific NDT methods that are already used on the Serbian railways (visual testing and conventional ultrasonic testing), as well as the methods recommended by the authors of this paper, as follows:
  − ultrasonic testing using phased array probes,
  − conventional eddy current testing, and
  − axle box acceleration measurement.

SWOT analysis was used to see if the suggested NDT methods would work on the Serbian railway network to find RCF rail defects. This type of analysis gives a full picture of a thing's strengths, weaknesses, opportunities, and threats (Table 3). Considering these methods' advantages, their high precision in detecting structural changes indicative of RCF defects stands out. Additionally, their effectiveness in

identifying defects at the early stages of development enables preventive maintenance, which can significantly reduce costs and enhance overall railway system safety.

However, these methods are not without objective and/or subjective limitations. High implementation costs, particularly the acquisition of specialized equipment and personnel training, are possible weaknesses. Limitations in inspection speed and data analysis complexity may also pose challenges. Opportunities for improvement in these methods may arise from technological advancements and the development of algorithms for rapid and precise result analysis.

Furthermore, the SWOT analysis recognises opportunities for integrating new technologies, such as artificial intelligence (AI) and machine learning, to enhance the efficiency and precision of RCF defect detection. Opportunities also exist for the development of standardised inspection procedures to ensure consistency in the application of these methods globally, with the possibility of combining several NDT methods.

On the other hand, threats may stem from insufficient support for research and the implementation of new technologies, as well as the rapid technical obsolescence of existing equipment. Therefore, despite challenges, the SWOT analysis provides a comprehensive overview to optimize the use of proposed methods for NDT inspection of rail RCF defects, contributing to the improvement of safety and sustainability in railway systems.
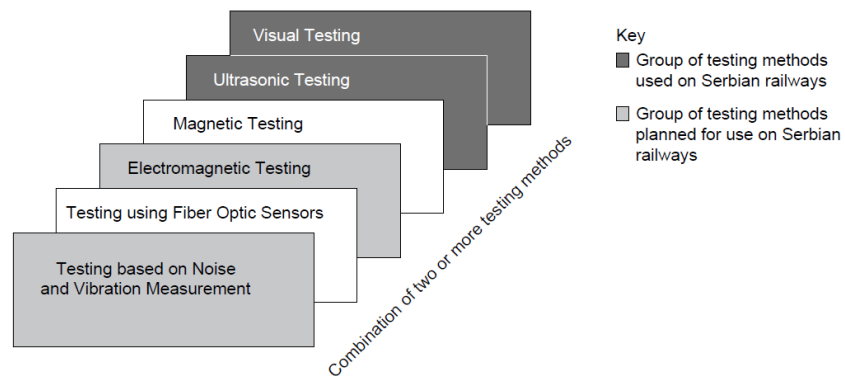

Figure 6. Available, used, and recommended groups of NDT methods for the inspection of RCF rail defects on the Serbian railway network
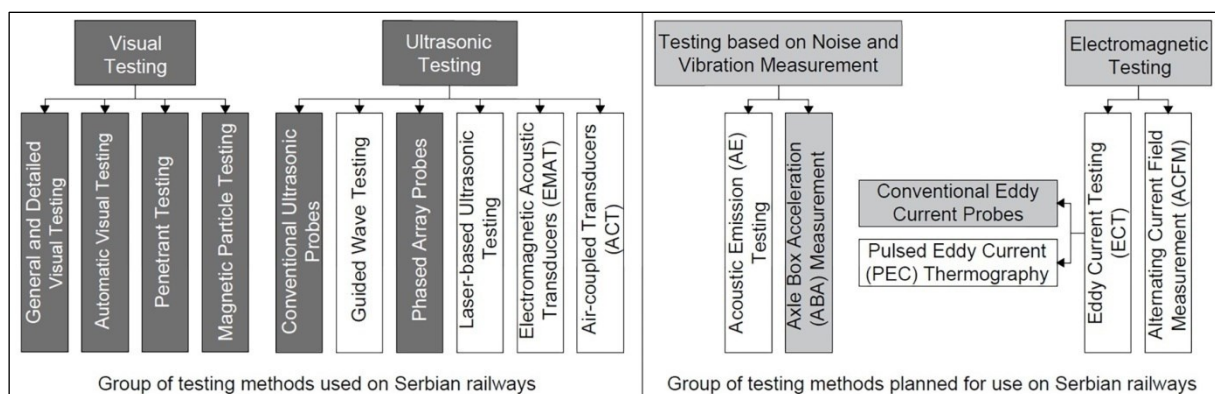

Figure 7. NDTs used (left) and recommended for use(right) on the Serbian railway network

Table 3. SWOT analysis of recommended NDTs for RCF rail defects on the Serbian railway network

INTERNAL FACTORS		
☺STRENGTHS of recommended NDTs		☹WEAKNESSES of recommended NDTs

	STRENGTHS			WEAKNESSES
✓	Possibility of combining the proposed methods (VT, AVT, MT, PT, conventional UT, phased array UT, ECT, ABA).		?	Obligation of IM to organize test track sections for calibration of measuring systems mounted on measuring vehicles and training of professional staff (conventional UT, phased array UT, ECT, ABA).
✓	Possibility of mounting measuring equipment on the SEVER-1435 track recording car (Figure 8) used by Serbian Railways (AVT, phased array UT, ECT, ABA).		?	Inability to apply the method in bad weather conditions (VT, AVT, MT, PT).
✓	Possibility of installing measuring equipment on commercial and inspection vehicles at commercial speed (AVT, ABA).		?	Inability to detect defects undercertain sizes(VT, AVT, conventional UT, phased array UT, ABA).
✓	Detection of defects in the early development stage (phased array UT, ECT, ABA).		?	Inability to detect defects over acertain size (conventional UT, phased array UT, ECT).
✓	Evaluation of defect severity (VT, AVT, ABA).		?	Inabilityof theNDT method to detect RCF subsurface rail defects (VT, AVT, conventional UT, ABA).
✓	Accessibility and usability of the inspection method (AVT, MT, conventional UT, phased array UT, ECT, ABA).		?	Inability to assess the severity of RCF defects(MT, PT, conventional UT, phased array UT, ECT).
✓	Simplicity inthe interpretation of inspection results (VT, AVT, conventional UT, phased array UT, MT, PT, ECT, ABA).		?	Inspectionand measurement of RCF rail defects obscured by other cracks (UT, AVT, ECT).
✓	Application ofNDT method on running rails(AVT, conventional UT, phased array UT, ECT, ABA), preferably without track closure.		?	The pronounced subjectivity in assessing the type and severity of RCF rail defect (VT, AVT).
✓	Mounting of inspection equipment to the inspection trolley for testing specific zones of limited length (AVT, conventional UT, phased array UT, ECT, ABA), preferably without track closure.		?	Impossibility to mount to the commercial and/or inspection vehicle (VT, MT, PT).
			?	Low inspection speed and application of the method on track sections of limited length (VT, MT, PT).
✓	Application of non-contact NDT methods (ABA, AVT, ECT).		?	Safety risk for persons who are conducting inspections (VT, MT, PT, all types of inspections using trolley).

EXTERNAL FACTORS		
☺ OPPORTUNITIESforrecommended NDTs		☹THREATSfor recommended NDTs

	OPPORTUNITIES			THREATS
±	Education of inspection staff and improvement of knowledge in the field of RCF defect developmentthrough professional seminars in Serbia.		!	RCF defects are spread over the entire railway network (about 3800 km of railway lines in Serbia).
±	Specialized education for improving the knowledge of engineers for the application of inspection methods and analysis of measurement results with obtaining a certificate.		!	Lack of professional knowledge and experience among infrastructure maintenance employees in predicting the development of RCF defects.
			!	Availability of professional staff training and certification only abroad.
±	Combining the results of several methods to detect with greater probability the exact type (type and severity) and characteristics of defects.		!	Lack of professional knowledge and experience in rail maintenance planning (preventive, cyclical and corrective maintenance of running rails in service).
±	Further improvement of NDT inspection methods.		!	Reliance on the rail inspection schedule based on railway traffic timetables.
±	Automated identification and classification of RCF rail defects based on their type and severity using AI.		!	Possibility to conduct rail inspection within short periods of railway line closure.
±	Development of machine learning techniques suitable for defect detection.		!	Reluctance of the inspection management to embrace innovative inspection technologies.
±	Expanding the database of individual defects used for AI training.		!	High costs forpurchase and maintenance of inspection equipment.

± Optimizing the number and type of parameters for detecting defects using machine learning.	! Impossibility to calibrate and verify the operation of the equipment according to the prescribed cycles at test sections/laboratories.
± Support provided by EN standardisation of NDT inspection method.	! Undetected RCF rail defects may impact the safety of railway operations.
± Improving railway transport sustainability and competitiveness in Serbia by ensuring safety, increasing comfort, reducing maintenance costs, andreducing noise and vibration emissions.	! Challenges associated with the procurement of equipment from international sources based on the risk of availability of materials and components.
± Establishing a laboratory for periodic calibration and checking the characteristics of measuring equipment in Serbia.	
Key: ABA - Axle Box Acceleration, AVT - Automatic Visual Testing ECT - Eddy Current Testing	MT - Magnetic Particle Testing PT - Penetrant Testing UT - Ultrasonic Testing VT - Visual Testing

4 Advantages and limitations of the proposed NDTs

In their previous paper [2], the authors provided a comprehensive overview of modern NDT methods for the inspection of RCF rail defects. Before analysing which methods are suitable for application on the Serbian railway network, the expert team of the Serbian IM should have a good understanding of the procedures and equipment required for implementing these modern NDT methods. This paper highlights the advantages and limitations of each of the proposed methods without delving into the details of the procedures and equipment required for implementing them.

4.1 General and detailed visual testing (VT) and automatic visual testing (AVT)

For years, the Serbian railways relied on maintenance workers to visually inspect tracks in service. Visual examination of rail surface conditions by qualified railway personnel walking along the tracks is the most basic method for general and detailed testing. However, this approach has several drawbacks: it is slow, subsurface and internal defects cannot be observed, it poses safety risks for personnel, and it heavily relies on the knowledge and experience of the railway personnel conducting the inspection [21, 22]. To avoid these issues, the European standard [4] recommends a comprehensive visual testing approach for assessing rail corrugation and other surface rail defects using auxiliary lighting to ensure adequate illumination, enabling a thorough inspection and evaluation of track conditions.

The VT methods provide information on visible surface rail defects. The advantages of this method include its simplicity, which provides a direct insight into the rail surface condition. Moreover, VT can be utilized to control and verify the results from other inspection methods.

Inspection results may be subjective, and a combination of VT and AVT methods is often required for comprehensive analysis. VT has limitations in detecting defects at an early stage of development, and its performance is constrained by the need for walking the track the track, limiting inspection to shorter track sections. Weather conditions and traffic management during rail inspection also influence VT

outcomes, and the presence of grinding marks can obscure surface defects in their early stages.

As the speed of commercial trains has increased, reaching up to 200 km/h on the Belgrade-Novi Sad line, and the density of railway traffic has grown, the traditional visual method for detecting irregularities on the rail surface has lost some of its importance. However, automation of visual testing plays a crucial role in quickly and efficiently identifying rail surface irregularities. In Serbia, AVT equipment is mounted on an inspection car (Figure 8). The AVT system includes a device for illumination of running rails, a digital camera, and a device for image processing and defect identification. A specially designed illumination system ensures the preservation of a clear and contrasted image in any weather condition and at any time of the day [23].

AVT is a significant method for detecting surface defects, including squat, HC, belgrospi, and surface corrugation. This method involves various defect parameters, focusing on the precise location, area and length of surface deformation (squat, belgrospi), surface crack length and visibility of subsurface cracks indicated by dark patches on the rail surface (HC), defect orientation, number, and the assessment of defect severity.

The AVT system is an automated inspection system that is user-friendly and simple to operate. The method relies on high-resolution cameras, and its effectiveness is influenced by weather conditions. The AVT method is suitable for real-time monitoring and more detailed determination of defect parameters through image post-processing. However, this method's outcomes may still be influenced by subjectivity, and the presence of grinding marks can obscure surface defects at an early stage of development. A combination of the VT and AVT methods is often required for comprehensive defect analysis.

Limitations on measurement speeds stem from the impact of higher vehicle speeds on image blurring. Detailed inspections are feasible at lower speeds, while inspections at higher speeds rely on the jump search method [24].

To improve efficient rail inspection, ongoing developments of the AVT method focus on more detailed image processing and real-time inspection using complex algorithms [25-28].

Figure 8. Modern recording car for track inspection on the Serbian railway network

4.2 Magnetic particle testing (MT) and penetrant testing (PT)

MT and PT constitute suitable methods for detecting surface defects, including squat, belgrospi and HC, on short track sections. These methods primarily focus on defect parameters such as location and surface crack length, although the latter is rarely utilized for squat defects.

Noteworthy advantages of these methods include the ability of MT to indicate the presence of shallow subsurface defects, albeit with insufficient reliability [29]. Both MT and PT offer improved visibility of small defects at an early stage of development compared to VT and AVT. Additionally, these methods provide the possibility of recognizing defects below contaminated surfaces, such as those affected by lubricants. However, both MT and PT have inherent disadvantages, as they are not automatic and are time-consuming.

4.3 Ultrasonic testing (UT) using conventional and phased array ultrasonic probes

Calibration of the measuring system for volume defects is described in EN 16729-1 [30]. It defines the methods for calibrating probes and the preparation of the test sections. Furthermore, in [30], the optional and mandatory probe angles for different types of volumetric rail defects, as well as the frequency range of ultrasonic waves (from 2 to 5 MHz), are defined.

In addition, standard EN 16729-3 [4] indicates the possibility of using UT probes for the detection of certain types of RCF defects (HC and squat, excluding corrugation and belgrospi), by defining the probe angle and the way of conducting the inspection (manual or vehicle-mounted equipment).

In general, the conventional UT method may prove incapable or unreliable in detecting surface and shallow subsurface defects due to the "dead-zone" phenomenon. The width of this zone depends on the probe angle concerning the vertical plane defined by [4] and affects the minimum depth at which defects can be detected. Furthermore, the minimum depth of defect detection is different depending on whether manual or vehicle-mounted equipment is used.

To detect squat and HC defects, it is recommended to use a probe angle of 70° to excite subsurface Rayleigh waves in the rail head. Moreover, for measuring the depth of the squat depression, a probe angle of 0° is recommended. However, it is important to note that the measurements may be obscured by other local cracks. For manual UT of HC defects, vertical depth can only be measured from 3 mm. In the case of vehicle-mounted UT equipment for HC defects, vertical depth measurement starts from 5 mm [4].

Instead of conventional UT, the application of phased array probes is increasing. The advantage of these probes lies in the capability of software to adjust the frequency, angle, and penetration depth of ultrasonic waves to specific appearance zones associated with rail defects. It allows for the simultaneous spreading of ultrasonic waves in various directions. One phased array probe can replace seven conventional UT probes, which reduces the amount of contact medium needed for inspection. Phased array systems enable fast signal analysis, and the real-time defect detection algorithms are constantly being improved.

The method's speed limitations stem from the influence of the contact medium and the needed measurement resolution. Modern measuring systems have developed protection for the probes from wear based on different forms of belts and sliding systems. In practice, inspection at speeds up to 80 km/h provides accurate detection of defects. The preferable inspection speed range is from 40km/h to 80 km/h, although some manufacturers provide systems intended for speeds up to 100 km/h.

4.4 Eddy current testing (ECT) using conventional probes

ECT, particularly when employing conventional eddy current probes, represents an efficient and often used method for detecting both surface-originated and subsurface defects like squat, HC, flaking, and spalling [4, 31]. It is a non-contact inspection method and can be optimised for specific types and zones of defect by choosing optimal shapes, characteristics, and arrangements of eddy current probes. This is the standard inspection method implemented both on commercial manual systems and automatic systems mounted on vehicles. The defect parameters that can be detected are precise location, HC pocket length, depth (with limitations on accuracy), and distance between HC cracks. The authors presented a detailed description of this method in their published papers [2, 32].

ECT can be utilized to monitor the performance of rail grinding machines [33] and is suitable for combination with other inspection methods [34].

The disadvantage of this method is the influence of lift-off on the characteristics of eddy current signals [35]. This affects the accuracy of squat defect sizing andthe evaluation of the depth of HC cracks and their distance. Additionally, the depth of penetration of eddy currents is limited by the inspection material and used frequency, so the pocket length of HC defects can be measured up to 10 mm, and their depths are calculated indirectly using an assumed angle and the measured pocket length [4].

When eddy current systems are mounted on the vehicle, the vehicle speed causes an increase in the frequency of induced eddy currents and a change in their penetration depth. The usual measuring speeds are up to 80 km/h.

The accuracy of the method is improved by applying multi-differential eddy current probes and enhancing the signal processing techniques [36-39].

4.5 Tests using axle box acceleration (ABA) measurements

The ABA method uses accelerometers mounted on the axlebox of trains in-service to determine the short- and long-wave unevenness of the rail head surface. This system detects vertical and longitudinal oscillations due to rail surface defects [40]. Signal processing is based on frequency and time domain analysis of ABA signals, including wavelet analysis.

This method represents a significant method for detecting squats and corrugation, and commercial ABA systems are applied worldwide [41]. It focuses on defect parameter evaluation, such as the exact location and length of surface depression. Additionally, this method is suitable for the automatic detection and classification of squat defect severity into four categories (trivial, light, moderate, and severe). Each defect severity category has characteristic amplitude-frequency spectra for ABA signals. Compared to vertical, longitudinal ABA signals are particularly sensitive to detecting light squats [42].

However, hunting, rolling bandwidth, and periodic repetitive vibrations originating from wheel defects influence the measured ABA signal and the probability of defect recognition. Moreover, the ABA signal characteristics of light squat defects are influenced by the speed of inspection vehicles and commercial trains.

5 Conclusion

This paper reports on the results of a case study that analysed the inspection methods used for identifying Rolling Contact Fatigue (RCF) rail defects on the railway network in Serbia, involving the performance of the railway infrastructure, inspection vehicles, and the expertise of the professional staff.

Effective inspection and maintenance of rail defects, particularly RCF rail defects, are crucial for ensuring the safety and reliability of railway networks. The implementation of standardized inspection methods, such as ultrasonic testing (UT), visual testing (VT), automatic visual testing (AVT), eddy current testing (ECT), magnetic particle testing (MT), and penetrant testing (PT), plays a significant role in identifying and monitoring various types of RCF rail defects. Furthermore, the utilization of advanced inspection methods and adherence to reference European standards are essential for enhancing the accuracy and efficiency of defect detection.

The Infrastructure Manager (IM) has to establish a comprehensive Rule book encompassing essential data for successful inspection and maintenance of rail defects, including standardized benchmark photos, detailed descriptions of defect origin and development, recommended inspection methods, and unique numbering codes.

Additionally, collaboration with international research initiatives and adherence to safety guidelines outlined by organizations such as the European Committee for Standardization (CEN) and the International Union of Railways (UIC) is fundamental for promoting best practices in rail defect management. Considering future developments in inspection technologies, it is recommended that the Railways of Serbia continue to invest in research of modern inspection methods for RCF rail defects. This includes exploring the potential of phased array technology, eddy current testing and axle box acceleration measurements for more efficient and comprehensive RCF defect detection. Furthermore, the establishment of a laboratory and test track section for periodic calibration and checking the characteristics of measuring equipment would further enhance the accuracy and reliability of inspection processes in Serbia.

The paper promotes the significance of combining different non-destructive inspection methods to provide reliable and early detection of RCF rail defects within the railway network. By integrating various inspection methods, it becomes possible to comprehensively assess the condition of the rails and identify RCF defects in their early stages. This approach not only contributes to the overall safety and reliability of railway operations but also minimises the potential impact of RCF defects on maintenance costs, noise, and vibration emissions.

By continuously refining inspection techniques and embracing technological advancements, the Railways of Serbia could mitigate the risks associated with RCF rail defects, ultimately ensuring the sustaining of the lifecycle and safety of the railway network for passengers and freight transportation.

Credit authorship contribution statement

Declaration of conflicting interests

The authors declare no potential conflicts of interest with respect to the research, authorship, and/or publication of this article.

Acknowledgement

Funding

References

[1] Z. Popović, L. Lazarević, The role of railway in the European transport policy, Izgradnja 67(7-8) (2013) 285-291.

[2] M. Mićić, Lj.Brajović, L. Lazarević, Z.Popović,Inspection of RCF rail defects–Review of NDT methods, Mech. Syst. Signal Pr. 182 (2023)109568.https://doi.org/10.1016/j.ymssp.2022.109568.

[3] International Union of Railways, IRS 70712 Rail Defects, 2018.

[4] CEN, EN 16729-3:2018, Railway applications - Infrastructure - Non-destructive testing on rails in track - Part 3: Requirements for identifying internal and surface rail defects.

[5] CEN, EN 13231-5:2018, Railway applications - Track - Acceptance of works - Part 5: Procedures for rail reprofiling in plain line, switches, crossings and expansion devices.

[6] Z. Popović, L.Lazarević, M.Mićić, Lj.Brajović, Critical analysis of RCF rail defects classification, Transportation Research Procedia 63(2022) 2550-2561. https://doi.org/10.1016/j.trpro.2022.06.294.

[7] International Union of Railways, UIC Code 712 Rail defects, 2002.

[8] International Union of Railways, UIC Code 725 Treatment of rail defects, 2015.

[9] Office of Rail Regulation, Train derailment at Hatfield: A final report by the independent investigation board. https://www.railwaysarchive.co.uk/documents/HSE_HatfieldFinal2006.pdf, 2006 (accessed 10 January 2024).

[10] E. Magel, P. Mutton, A. Ekberg, A. Kapoor, Rolling contact fatigue, wear and broken rail derailments, Wear 366 (2016) 249-257. https://doi.org/10.1016/j.wear.2016.06.009.

[11] Z. Popović, V. Radović, Analysis of cracking on running surface of rails, Gradevinar 65(3) (2013) 251-259. https://doi.org/10.14256/JCE.877.2012.

[12] M. Ishida, Rolling contact fatigue (RCF) defect of rails in Japanese railways and its mitigation strategies, Electron. J. Struct. Eng. 13 (1) (2013) 67–74.https://doi.org/10.56748/ejse.131621.

[13] Z. Popović, Lj. Brajović, L. Lazarević, L. Milosavljević, Rail defects head checking on the Serbian railways, Teh. Vjesn. 21(1) (2014) 147-153. https://hrcak.srce.hr/116587.

[14] R. Heyder, M. Brehmer, Empirical studies of head check propagation on the DB network, Wear 314(1-2) (2014) 36-43. https://doi.org/10.1016/j.wear.2013.11.035.

[15] M. Vilotijević, Lj. Brajović, A. Pustovgar, Methodology for statistical analysis of squat rail defects, in: XVIII Scientific-expert conference on railways-RAILCON 18, Faculty of Mechanical Engineering, Niš, Serbia, 2018, pp. 157-160.

[16] M. Ishida, History of mitigating rolling contact fatigue and corrugation of railway rails in Japan-Review, EPI Int. J. Eng. 1(2) (2018) 13-24.https://doi.org/10.25042/epi-ije.082018.02.

[17] V.V. Krishna, S. Hossein-Nia, C. Casanueva, S. Stichel, Long term rail surface damage considering maintenance interventions, Wear 460–461 (2020) 203462.https://doi.org/10.1016/j.wear.2020.203462.

[18] H. Zhu, H. Li, A. Al-Juboori, D. Wexler, C. Lu, A. McCusker, J. McLeod, S. Pannila, J. Barnes, Understanding and treatment of squat defects in a railway network, Wear 442 (2020) 203139.https://doi.org/10.1016/j.wear.2019.203139.

[19] S.Y. Zhang, M. Spiryagin, H.H. Ding, Q. Wu, J. Guo, Q.Y. Liu, W.J. Wang, Rail rolling contact fatigue formation and evolution with surface defects, Int. J. Fatigue 158 (2022) 106762.https://doi.org/10.1016/j.ijfatigue.2022.106762.

[20] W. Schoech, Rolling contact fatigue mitigation by grinding, in: Proceedings of the Rail Tech Europe Conference, Utrecht, 2007.

[21] Y. Santur, M. Karaköse, E. Akin, Random forest based diagnosis approach for rail fault inspection in railways, in: 2016 National Conference on Electrical, Electronics and Biomedical Engineering (ELECO 2016), Bursa, Turkey, 2016, pp. 745-750.

[22] Z. Popović, V. Radović, L. Lazarević, V. Vukadinović, G. Tepić, Rail inspection of RCF defects, Metalurgija 52(4) (2013) 537-540. https://hrcak.srce.hr/100836.

[23] Tvema. https://tvema.com/640, (accessed 10 January 2024).

[24] F. Marino, A. Distante, P.L. Mazzeo, E. Stella, A real-time visual inspection system for railway maintenance: automatic hexagonal-headed bolts detection, IEEE T. Syst. Man Cy. C 37(3) (2007) 418-428. https://doi.org/10.1109/TSMCC.2007.893278.

[25] Y. Min, B. Xiao, J. Dang, B. Yue, T. Cheng, Real time detection system for rail surface defects based on machine vision, EURASIP J. Image. Vide. 2018 (1) (2018) 3, https://doi.org/10.1186/s13640-017-0241-y.

[26] D. De Becker, J. Dobrzanski, L. Justham, Y. Goh, A laser scanner based approach for identifying rail surface squat defects, P. I. Mech. Eng. F-J. Rai. 235 (6) (2021) 763–773, https://doi.org/10.1177/0954409720962252.

[27] J. Ye, E. Stewart, C. Roberts, Use of a 3D model to improve the performance of laser-based railway track inspection, P. I. Mech. Eng. F-J. Rai. 233 (3) (2019) 337–355, https://doi.org/10.1177/0954409718795714.

[28] Y. Wu, Y. Qin, Z. Wang, L. Jia, A UAV-based visual inspection method for rail surface defects, Appl. Sci. 8 (7) (2018) 1028, https://doi.org/10.3390/app8071028.

[29] N. Pedrosa, M. Pinto, M. Papaelias, INTERAIL - Towards a safer and reliable European Railway, in: Transport Research Arena (TRA) 5th Conference: Transport Solutions from Research to Deployment, Paris, France, 2014, 10 pp.

[30] CEN, EN 16729-1:2016, Railway applications - Infrastructure - Non-destructive testing on rails in track - Part 1: Requirements for ultrasonic inspection and evaluation principles.

[31] CEN, EN 16729-2:2020, Railway applications - Infrastructure - Non-destructive testing on rails in track - Part 2: Eddy current testing of rails in track.

[32] Z. Popović, Lj. Brajović, L. Lazarević, Rail inspection by eddy current method, in: 3rd International Scientific and Professional Conference „CORRIDOR 10 - A sustainable way of integrations", Belgrade, Serbia, 2012, pp. 238-251.

[33] R. Pohl, R. Krull, R. Meierhofer, A new eddy current instrument in a grinding train, in 9th European Conference on NDT, Berlin, Germany, 2006, pp. 1-7. https://www.ndt.net/article/ecndt2006/doc/P178.pdf

[34] T. Szugs, A. Krüger, G. Jansen, B. Beltman, S. Gao, H. Mühmel, R. Ahlbrink, Combination of ultrasonic and eddy current testing with imaging for characterization of rolling contact fatigue, in: 19th World Conference on Non-Destructive Testing (WCNDT 2016), Munich, Germany, 2016, vol. 2, pp. 1603-1610. https://www.wcndt2016.com/Programme/show/P22.

[35] J. Rajamaki, M. Vippola, A. Nurmikolu, T. Viitala, Limitations of eddy current inspection in railway rail evaluation, P. I. Mech. Eng. F-J. Rai. 232 (1) (2016) 121–129, https://doi.org/10.1177/0954409716657848.

[36] A. Opanasenko, A. Iurchenko, G. Lutsenko, V. Uchanin, Eddy current multi-channel module for in-line high-speed inspection of railroad rails, in: 19th World Conference on Non-Destructive Testing (WCNDT 2016), Munich, Germany, 2016, vol.6, pp. 4478-4484, https://www.wcndt2016.com/Programme/show/P98.

[37] V. Uchanin, New type multidifferencial eddy current probes for surface and subsurface flaw detection, in: ZeszytyproblemoweBadanianieniszczące, Warsaw, Poland, 2001, no. 6, pp. 201-204.

[38] S.G. Kwon, T.G. Lee, S.J. Park, J.W. Park, J.M. Seo, Natural rail surface defect inspection and analysis using 16-channel eddy current system, Appl. Sci. 11 (17) (2021) 8107, https://doi.org/10.3390/app11178107.

[39] J.W. Park, T.G. Lee, I.C. Back, S.J. Park, J.M. Seo, W.J. Choi, S.G. Kwon, Rail surface defect detection and analysis using multi-channel eddy current method based algorithm for defect evaluation, J. Nondestruct. Eval. 40 (2021) 83, https://doi.org/10.1007/s10921-021-00810-9.

[40] M. Molodova, Z. Li, A. Núñez, R. Dollevoet, Automatic detection of squats in railway infrastructure, IEEE T. Intell. Transp. 15 (5) (2014) 1980–1990, https://doi.org/10.1109/TITS.2014.2307955.

[41] H. Cho, J. Park, K. Park, Analysis of axial acceleration for the detection of rail squats in high-speed railways, CivilEng 4(4) (2023), 1143-1156, https://doi.org/10.3390/civileng4040062

[42] Z. Li, M. Molodova, A. Núñez, R. Dollevoet, Improvements in axle box acceleration measurements for the detection of light squats in railway infrastructure, IEEE T. Ind. Electron. 62 (7) (2015) 4385–4397, https://doi.org/10.1109/TIE.2015.2389761.

Technical paper

The impact of pier height on the construction costs of integral road bridges: An application of artificial intelligence

Željka Beljkaš[*1)], Miloš Knežević[2)]

[9)] *Faculty of Civil Engineering, University of Montenegro, Podgorica 81000, Montenegro. ORCID 0000-0002-1648-9512*
[10)] *Faculty of Civil Engineering, University of Montenegro, Podgorica 81000, Montenegro. ORCID 0000-0002-4952-9699*

A B S T R A C T

There are multiple definitions for integral road bridges. One of them explains that these are single-span bridges without expansion joints or bearings at the discontinuity locations. In terms of durability and maintenance, discontinuity locations are considered to be construction parts most exposed to damage in this type of structure. Engineers' efforts to lower maintenance costs and extend the durability of structures have led to the emergence of integral bridges. Early assessment of construction costs is crucial in determining the justification for constructing such structures, as it allows both the investor and the contractor to gauge their involvement in the project's implementation. The construction costs can be determined based on the structure characteristics. One of the major characteristics of integral bridges is the height of their piers. This paper examines how the pier height affects the construction costs of integral road bridges. The prognostic model in the Python 3.7.6 software package applies neural networks to determine the impact of pier height. According to the research, the pier height accounts for up to 20% of the total construction costs of integral road bridges.

1 Introduction

Each structure is unique and has its own specificities. Many factors influence the construction costs of these structures. An estimate of the cost for each of the structures implies quantification of all the elements or resources that are an integral part of the construction and which are necessary for its completion. Determining the impact of any of the elements participating in the total sum is particularly challenging in the early stages of the project.

Numerous definitions exist for integral road bridges. These are single-span structures with no expansion joints or bearings at the discontinuity locations. Moreover, these bridges represent a continuous frame without expansion joints and bearings only above the medium piers. For this type of bridge, the engineers also use the name semi-integral bridges.

This type of bridge is easier to maintain, experiences fewer damages, has a longer lifespan, and enhances traffic safety. The primary cause of damage stems from discontinuity locations, which are either non-existent or absent in these bridges situated over medium piers. These bridges are constructed in monolithic, or prefabricated-monolithic, style.

The integral bridges consist of the span structure, piers, and bridge equipment. Each of these parts generates certain costs during the construction process. As the project progresses, the quantity and quality of data relating to bridge parts change. At the onset of project implementation, there is a limited amount of information available, and its reliability is lower. However, the possibility of an impact on expenses is the greatest in these early stages of project implementation. The impact on expenses decreases as the project progresses (Figure 1). The information we have allows us to accurately determine the impact of each factor on the cost. This is why determining the impact of any factor on the total cost of construction at an early stage of bridge realisation presents a greater challenge.
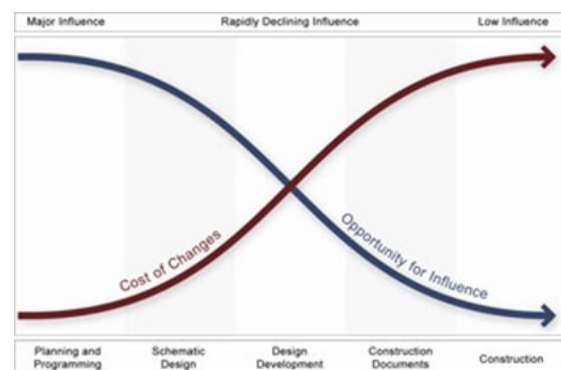

Figure 1. Cost-effective time to make changes [1]

---

[*] Corresponding author:
   E-mail address: zeljkab@ucg.ac.me

This study demonstrates the effect of pier height on the cost of building integral road bridges The defined prognostic model for construction cost estimation has been used for analyzing the impact.

1.1 Application of artificial neural networks in construction

The publication of Adeli and Yeh's work [2] in the journal Microcomputers in Civil Engineering in 1989 marked the beginning of the application of neural artificial networks in construction. From its inception until today, the application of neural networks has grown. The reason for their wide application lies, on the one hand, in the wide range of possibilities they have and, on the other hand, in the very rapid development of software packages that provide users with a more comprehensive application.

One possible application of neural networks in civil engineering is to define prognostic models to estimate the cost of different types of building structures. There are a large number of papers in the literature that present different models for cost estimates [3, 4, 5, 6, 7, 8, 9, 10, 11].

M. O. Sanni-Anibire, R. M. Zin, and S. O. Olatunji developed a model for estimating the cost of building construction structures in the early stages of the project using artificial intelligence techniques. The authors defined 12 models and determined their performances. The authors present the performances using Root Mean Squared Error (RMSE =6.09) and Mean Absolute Percentage Error (MAPE = 80.95%) [12].

S. Nirajkumar, J. P. Shah, Z. H. Shah, and M. S. Holia focused their research on estimating the costs of the structures that are part of the road infrastructure during the early design stages. The research resulted in the identification of appropriate factors that are easily available in the early stage and are used for fast, simple, and accurate enough cost estimates [13].

S. K. Magdum and A. C. Adamuthe developed a prognostic model for estimating construction costs. Four models of neural networks (NN) and 12 multi-layered perceptron models (MLP) were compared. MLP and NN give better results than the statistical regression methods. Compared to NN, MLP functions better on a training data set, which is not the case with a test set. Five functions for activation were tested to identify an appropriate function for the problem. The "Elu" activation function gives better results than other activation functions. The study showed that the RMSE values for multiple linear regressions, NN, and MLP were 62.6269, 41.69, and 28.49, respectively. MLP performance is better than that of NN and statistical multiple regression [14].

G. H. Kim, S. Hoon An, and K. Kang examined the performance of three cost estimation models. The trials were based on multiple regression analysis (MRA), neural networks (NN), and case-based reasoning (CBR) using 530 cost data points. NN provided the best estimation model compared to MRA or CBR estimation models. On the other hand, the CBR estimation model outperformed the NN estimation model in terms of long-term use, available results information, and time-to-accuracy ratios [15].

2 Materials and Methods

To consider the impact of the pier height on the cost of the construction of integral road bridges, a model was defined for estimating the estimated construction expenses.

The process of defining the prognostic model involved a number of steps. Figure 2 illustrates the stages involved in defining the model.
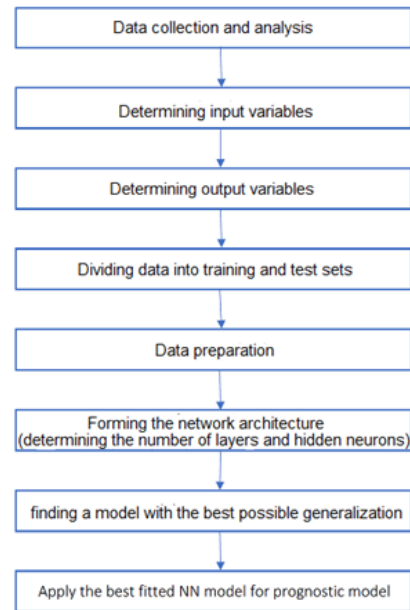
Figure 2. Stages in defining a prognostic model

The 101 main designs of integral road bridges built in the territories of Montenegro (48), Bosnia and Herzegovina (29), and Serbia (24), provide the data used to define a prognostic model. [16]

All the required data were analyzed from the bill of quantities and cost estimates of all the designs. Because the designs were made in three different countries and their forms differed, unifying data was required. To overcome differences, the same types of work were taken from the bill of quantities and cost estimates.

The next stage represents determining input variable models. The criteria for choosing input variables was their impact on the cost of the integral road bridge construction. Research has established that the Pareto distribution governs the behavior of reinforcing and concrete works, indicating their significant and costly nature. Based on this, we selected bridge design characteristics such as bridge length, bridge width, bridge pier height, and bridge span to directly influence cost. In addition to these, as the input variables of the model, the building technology and foundation method were taken, since it is known that they greatly influence the formation of the construction price.

Table 1 shows the input variables of the model with their minimum, maximum, and mean values. The bridges' lengths range from 11.5 to 784.4 m. The bridges are 6.5 to 30.55 m wide. The variable "pier height" represents the mean value of all the piers, and the bridge span implies the mean value of all spans. For the input variable "Construction technology" the following values are assigned: 0.25, 0.5, 0.75, and 1, depending on the pier height. The input variable "Foundation" has been assigned values 0, 1, and 2 depending on the founding methods, which are: 0 in the case of shallow foundation, 1 in the case of deep foundation, and 2 in the case of combined foundation.

Table 1. Input data[11,16]

No input data	Input data description	Data type	Measurement unit	Min	Max	Mean value
Input 1	Bridge length	numerical	m	11.5	784.4	153.25
Input 2	Bridge width	numerical	m	6.5	30.55	11.52
Input 3	Pier height	numerical	m	2.8	35.9	**13.65**
Input 4	Bridge span	numerical	m	11.3	44.5	24.07
Input 5	ConstructionTechnology	discrete	-	0	1	-
Input 6	Foundation	discrete	-	0	2	-

.

In addition to defining input variables, it was necessary to determine output variable models. Since the research aimed to define the impact of pier height on the price of the construction of integral road bridges, it is necessary to predict the cost of construction. Based on that, it has been determined that the output variable is the construction cost of integral road bridges (Table 2).

All the data were then divided into training and test sets. Apart from recommendations from the literature [17], we determine the number of data sets for each of these two sets based on the unique nature of the problem we are solving. In defining this model, the percentage ratio of data belonging to the training set to the test set was determined to be 70% to 30%. We selected data for the training and test sets in two ways: directly and through cross-validation procedures. Cross-validation procedures randomly selected the data.

It is necessary to prepare the data for entry into the software after dividing the data into two sets. Data preparation represents their transformation into quantities that are within a certain range. The literature [18] provides several methods for data transformation. The data transformation methods used in this study are Standard Scalar (Z-score normalisation) and Min-max normalisation.

Determining the network architecture means determining the number of layers and the number of neurons in each layer. Only one hidden number is enough to solve almost all the problems [19]. Several criteria exist for determining the number of neurons [19].

• The number of hidden neurons should be in the range between the size of the output layer and the size of the input layer $n_i < n_h < n_o$ (1)

• The number of hidden neurons should be equal to the sum of 2/3 of the size of the input layer and the size of the output layer $n_h = 2/3 * n_i + n_o$ (2)

• The number of hidden neurons should be smaller than the double size of the input layer $n_h < 2 * n_i$ (3)
where n_i represents the number of neurons in the input layer, n_o is the number of neurons in the output layer, and n_h is the number of neurons in the hidden layer.

After determining the network architecture, the next step involves identifying a model with good generalization, i.e., a model that produces sufficiently precise results based on unknown data. The model has a good possibility of generalisation when the predicted deviations from the expected results are small.

During the training of the model, its accuracy of prediction is constantly checked, i.e., model performance is measured. The performance of the models in this study was measured via MAE (Mean Absolute Error).

The Python 3.7.6 software package formed the prognostic model. We created a Multi-LayerPerceptrone MLP (Multi-LayerPerceptrone) to define the model.

Activation functions that are used for defining models are: for hidden neurons – the Rectified linear unit function (ReLu), hyperbolic tangent (tanh), and Swish, and for output neurons, the identity function was used (Table 3).

After selecting a model with the best performance, the final model is trained and recorded, and based on that, the prognostic model is defined for estimating the construction price of integral road bridges.

Table 2: Output variable of the model [11]

No of output data	Output data description	Data type	Measurement unit	Min	Max	Mean value
Output 1	Construction cost	numerical	€/m²	409.63	1752.36	915.97

Table 3. Activation functions of a multilayer perceptron model of an artificial neural network [18]

Function	Mark	Explanation	Range
Identity	x	Only in the output layer	$(-\infty, +\infty)$
Rectified Linear units	$max(0, x)$	The activation of neurons is transmitted directly as an output if it is positive, and if it is negative, 0 is transmitted. It has been proven to have six times better convergence compared to the hyperbolic tangent function.	$(0, +\infty)$
Hyperbolic tangent	$\dfrac{2}{(1 + e^{-2x})} - 1$	Activation of neurons is transmitted directly as an output if it is positive and if it is negative 0 is transmitted.	$(-1, 1)$
Swish	$x * sigmoid(x)$	A function that is nonlinearly interpolated between a linear and a ReLu function	$(0, x)$

3   Results and Discussion

Models of artificial neural networks are defined, taking into account all the necessary parameters. We adopted the network architecture based on the above recommendations. All neural networks have one input, one hidden, and one output layer. In the input layer of the network, they have six input variables, i.e., six neurons, and one output variable in the output layer, i.e., one neuron. Based on expressions (1), (2), and (3), the hidden layer adopted a maximum number of hidden neurons of five (Table 4).

The training results and characteristics of the artificial neural network models that showed the best performance are given in Tables 5 and 6.

For random choice of data, Cross-validation methods are used (kFold-CrossValidation and LeaveOneOut-CrossValidation - LOOCV). The values of model performance measures that gave the best results, as well as their characteristics are given in Tables 7 and 8.

Table 4. Artificial neural network architecture

Description	Number
Number of hidden layers	1
Number of neurons in the input layer	6
Number of neurons in the output layer	1
Max number of neurons in a hidden layer	5

Table 5. Artificial neural network models for construction cost estimation (StandardScalar)

Model name	Model characteristics	Activation function of hidden layers	Activation function of output layer	MAETraining set [%]	MAE Test set [%]
NN1	MLP 6-3-1	ReLu	Identity	0.0922	0.0752
NN6	MLP 6-5-1	Tanh	Identity	0.0547	0.0855
NN7	MLP 6-3-1	Swish	Identity	0.0866	0.0677

Table 6. Artificial neural network models for construction cost estimation (Min-Max normalization)

Model name	Model characteristics	Activation function of hidden layers	Activation function of the output layer	MAETraining set [%]	MAE Test set [%]
NN12	MLP 6-5-1	ReLu	Identity	0.0873	0.0920
NN13	MLP 6-3-1	Tanh	Identity	0.0993	0.0963
NN18	MLP 6-5-1	Swish	Identity	0.0940	0.0865

Table 7. Artificial neural network models with random data selection for construction cost estimation (kFold-CrossValidation, k=10)

Model name	Data scaling procedure	Model characteristics	Activation function of hidden layers	Activation function of the output layer	MAE Test set [%]
NN21	StandardScalar	MLP 6-5-1	ReLu	Identity	3.84

Table 8. Artificial neural network models with random data selection for construction cost estimation (LOOCV)

Model name	Data scaling procedure	Model characteristics	Activation function of hidden layers	Activation function of the output layer	MAE-Training set [%]	MAE Test set [%]
NN23	Min-Max	MLP 6-4-1	ReLu	Identity	0.0839	0.0932

We selected the model with the highest accuracy and the best prediction performance after a comparative analysis of all results. This is the NN7 model. In this model, the data were transformed by the StandardScaler method. The number of hidden neurons is three. Figure 3 displays the neural network architecture. The activation function is called Swish. The prediction expressed through MAE has an accuracy of 0.0677.

The model with the highest accuracy was chosen to form the final model for estimating the cost of building integral road bridges, and based on it, prognostic models were defined.

Based on the finally developed prognostic model, the impact of the pier height on the integral road bridge construction price has been analysed (Figure 4).

The diagram shows that the variable "Pier height" accounts for about one fifth of the total construction price, or, in other words, about 20%.

From the diagram of the change in the price of construction depending on the height of the bridge piers (Figure 5), it is clear that the price of construction increases to a certain value of the pier's height. As the pier height increases, the construction costs do not significantly change.
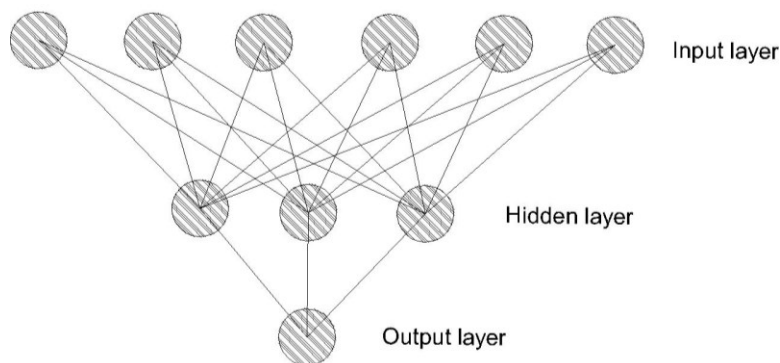

Figure 3. Artificial neural network architecture with the best performance
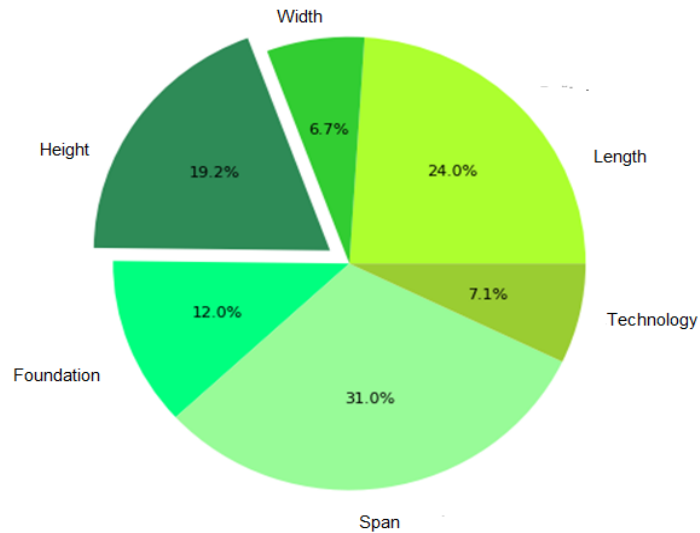
Figure 4. Impact of the input variable "Pier height" to the cost of integral road bridges construction
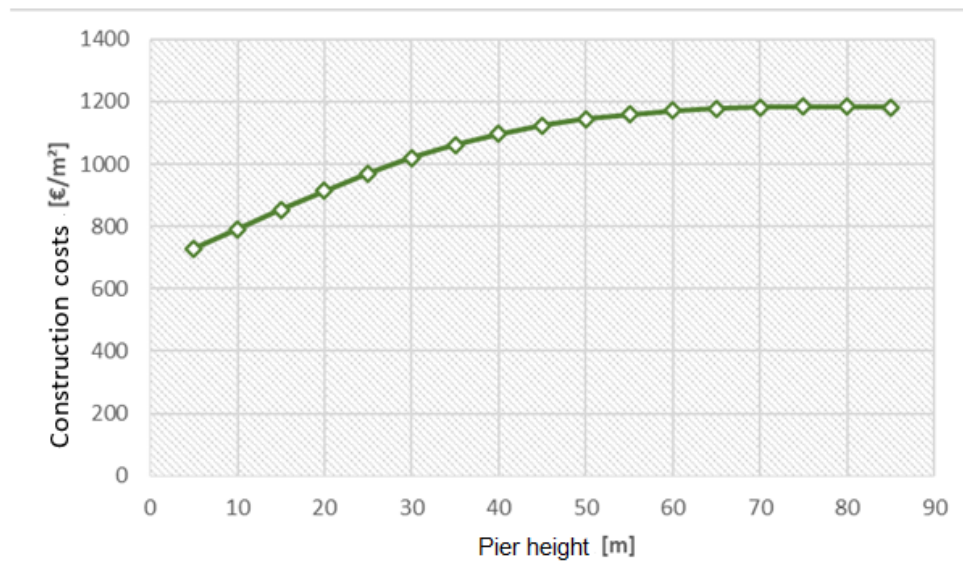

Figure 5. Change in the construction price depending on the pier height

4   Conclusions

The research results show that the model with the best performance is a model of an architecture of three layers: one input, one hidden, and one output layer. There are six neurons in the input layer, three neurons in the hidden layer, and one neuron in the output layer. The Swish function is the activation function of the hidden layer of neurons. The output layer has an activation function called Identity, i.e., a linear function. The mean absolute error (MAE) measured the prediction accuracy, and in the model with the best accuracy, it was 0.0677.

The prognostic model was defined based on the model that presented the best results in forecasting. Upon analysing the results and behaviour of a prognostic model, we observed that pier height accounts for 19.2% of the total sum. Furthermore, forecasts obtained in a specific case from the prognostic model indicate that the price of bridge construction has a growing trend until a certain pier height, and after that, the cost per meter square is slightly increasing.

The height of piers influences the choice of construction methods and technology. The piers can be cast in concrete in situ (depending on which types of piers they belong to, abutments or medium ones), or they could be made by using fixed, immovable, or sliding formwork. It is possible to incorporate the stated technologies for pier construction into the prognostic model, appropriately, and show the impact of the piers' height on the construction price. The results obtained in this way could be used to conduct a comparative analysis with the results of the model presented in this paper, thus determining the impact of the pier height on the price of bridge construction with even greater accuracy.

Author Contributions:

Conceptualization, Ž.B. and M.K.; Data curation, Ž.B; Formal analysis, Ž.B; Investigation, Ž.B.; Methodology, Ž.B. and M.K.; Project administration, Ž.B. and M.K.; Resources, Ž.B. and M.K.; Software, Ž.B.; Supervision, Ž.B. and M.K.; Validation, Ž.B. and M.K.; Visualization, Ž.B.; Roles/Writing—original draft preparation, Ž.B.; Writing—review and editing, Ž.B. and M.K.;

Conflicts of Interest:

The author declare that there is no conflict of interest regarding the publication of this paper.

References

[1] https://www.wbdg.org/design-disciplines/architectural-programming

[2] H. Adeli, C. Yeh, Perceptron learning in engineering design, Microcomputers in Civil Engineering, 4 (1989) 4, pp. 247–256, (1989).

[3] J. Sodikov, Cost estimation of highway projects in developing countries: artificial neural network approach, Journal of the Eastern Asia Society for Transportation Studies, Vol. 6, pp. 1036 - 1047, (2005).

[4] X. Wang, X. Duan, and J. Liu, Application of Neural Network in the Cost Estimation of Highway Engineering, Journal of Computers, Vol. 5, No. 11, (2010).

[5] C.G: Wilmont, and G. Cheng, Estimating Future Highway Construction Costs, Journal of Construction Engineering and Management Vol. 129 Issue 3 - June 2003, https://ascelibrary.org/doi/10.1061/%28ASCE%290733-9364%282003%29129%3A3%28272%29

[6] C.G Wilmont, and B. Mei, Neural Network Modeling of Highway Construction Costs, Journal of Construction Engineering and Management Volume 131 Issue 7 - July 2005, https://ascelibrary.org/doi/10.1061/%28ASCE%290733-9364%282005%29131%3A7%28765%29

[7] H.M. Gunaydin, and S.Z. Dogan, A neural network approach for early cost estimation of structural systems of buildings, International Journal of Project Management Volume 22, Issue 7, October 2004, Pages 595-602, https://www.sciencedirect.com/science/article/abs/pii/S0263786304000389

[8] Mehmet B.Kazez, and C.Vipulanandan, Bridge Damage and Repair Cost Estimates after a Hurricane, THC 2010 Conference& Exhibition.

[9] E. Atta-Asiamah, Estimation of the cost of building a water treatment plant and related facilities for Kaw City, Oklahoma, Faculty of the Graduate College of the Oklahoma State University, (2005).

[10] N. Fragkakis, S. Lambropoulos, and G. Tsiambaos, Parametric Model for Conceptual Cost Estimation of Concrete Bridge Foundations, Journal of Infrastructure Systems Volume 17 Issue 2 - June 2011, https://ascelibrary.org/doi/abs/10.1061/(ASCE)IS.1943-555X.0000044

[11] Ž.Beljkaš, and M.Knežević, Procjena koštanja integralnih mostova primjenom umjetne inteligencije, Građevinar 3/2021, DOI: https://doi.org/10.14256/JCE.2831.2019 ,(2021).

[12] M. O. Sanni-Anibire, R. M. Zin, and S. O. Olatunji, Developing a preliminary cost estimation model for tall buildings based on machine learning, Book Big Data and Information Theory, 1st Edition, eBook ISBN9781003289173, 2022, https://doi.org/10.4324/9781003289173

[13] S. Nirajkumar, J. P. Shah, Z. H. Shah, and M. S. Holia,A neural network approach to design reality oriented cost estimate model for infrastructure projects, RT&A, Special Issue № 1 (60) Volume 16, Janyary 2021.

[14] S.K.Magdum, and A.C.Adamuthe, Construction Cost Prediction Using Neural Networks, ICTACT Journal of Soft Computing October 2017, Vol 8, issue 1, https://doi.org/10.21917/ijsc.2017.0216

[15] G. H. Kim, S. Hoon An, and K. Kang, Comparison of construction cost estimating models based on regression analysis, neural networks, and case-based reasoning, Building and Environment, Volume 39, Issue 10, October 2004, Pages 1235-1242, https://doi.org/10.1016/j.buildenv.2004.02.013

[16] Ž.Beljkaš, M.Knežević, S.Rutešić, and N. Ivanišević, Application of Artificial Intelligence for the Estimation of Concrete and Reinforcement Consumption in the Construction of Integral Bridges, Hindawi Adv. Civ. Eng. Vol. 2020, ID 8645031, https://doi.org/10.1155/2020/8645031

[17] G. Zhang, B.E. Patuwo, and M.Y. Hu, Forecasting with artificial neural networks:The state of the art, Graduate School of Management, Kent State University, Kent, Ohio, USA, 1997.

[18] Ž.Beljkaš, and N.Baša, Neural Networks—Deflection Prediction of Continuous Beams with GFRP Reinforcement, Appl.Sci. 2021, 11, 3429. https://doi.org/10.3390/app11083429

[19] P.Gaurang, A.Ganatra, Y.P.Kosta, and D.Panchal, Behaviour Analysis of Multilayer Perceptronswith Multiple Hidden Neurons and Hidden Layers, International Journal of Computer Theory and Engineering, Vol. 3, No. 2, April 2011, ISSN: 1793-8201,https://doi.org/10.7763/IJCTE.2011.V3.328 (2021).

Building Materials and Structures

GUIDE FOR AUTHORS

In the journal *Building Materials and Structures*, the submission and review processes take place electronically. Manuscripts are submitted electronically (online) on the website **https: // www.dimk.rs.** The author should register first, then log in and finally submit the manuscript which should be in the form of editable files (e.g. Word) to enable the typesetting process in journal format. All correspondence, including Editor´s decision regarding required reviews and acceptance of manuscripts, take place via e-mail.

TYPES OF ARTICLES

The following types of articles are published in *Building Materials and Structures:*

Original scientific article. It is the primary source of scientific information, new ideas and insights as a result of original research using appropriate scientific methods. The results are presented briefly, but in a way to enable readers to assess the results of experimental or theoretical/numerical analyses, so that the research can be repeated and yield with the same or results within the limits of tolerable deviations.

Review article. It presents the state of science in particular area as a result of methodically systematized, analyzed and discussed reference data. Only critical review manuscripts will be considered as providing novel perspective and critical evaluation of the topics of interest to broader BMS readership.

Preliminary report. Contains the first short notifications of research results without detailed analysis, i.e. it is shorter than original research paper.

Technical article. Reports on the application of recognized scientific achievements of relevance to the field of building materials and structures. Contain critical analysis and recommendations for adaption of the research results to practical needs.

Projects Notes. Project Notes provide a presentation of a relevant project that has been built or is in the process of construction. The original or novel aspects in design or construction should be clearly indicated.

Discussions. Comment on or discussion of a manuscript previously published in *Building Materials and Structures*. It should be received by the Editor-in-Chief within six months of the online publication of the manuscript under discussion. Discussion Papers will be subject to peer review and should also be submitted online. If Discussion Paper is selected for publication the author of the original paper will be invited to respond, and Discussion Paper will be published alongside any response that the author.

Other contributions

Conference Reports. Reports on major international and national conferences of particular interest to *Building Materials and Structures*. Selected and/or awarded papers from the ASES Conferences are published in Special issues.

Book Reviews. Reviews on new books relevant to the scope of *Building Materials and Structures*.

PREPRINTS

These are the author's own write-up of research results and analysis that has not been peer reviewed, nor had any other value added to it by a publisher (such as formatting, copy-editing, technical enhancements and the like). Authors can share their preprint anywhere at any time. If accepted for publication, we encourage authors to link from the preprint to their formal publication via its Digital Object Identifier (DOI). Preprints should not be added to or enhanced in any way in order to appear more like, or to substitute for, the final versions of articles.

MANUSCRIPT STRUCTURE

The manuscript should be typed one-sided on A4 sheets. Page numbers should be included in the manuscript and the text should be single spaced with **consecutive line numbering** - these are essential peer review requirements. The figures and tables included in the single file should be placed next to the relevant text in the manuscript. The corresponding captions should be placed directly below the figure or table. If the manuscript contains Supplementary material, it should also be submitted at the first submission of the manuscript for review purposes.

There are no strict rules regarding the structure of the manuscript, but the basic elements that it should contain are: Title page with the title of the manuscript, information about the authors, abstract and keywords, Introduction, Materials / Methods, Results and Conclusions.

The front page

The front page contains the title of the manuscript which should be informative and concise; abbreviations and formulas should be avoided.

Information about the authors are below the title; after the author's name, a superscript number is placed indicating his/her affiliation, which is printed below the author's name, and before the abstract. It is obligatory to mark the corresponding author with superscript *) and provide his/her e-mail address. The affiliation should contain the full name of the institution where the author performed the research and its address.

Abstract

Abstract should contain 150-200 words. Motivation and objective of the conducted research should be presented; main results and conclusions should be briefly stated as well. References and abbreviations should be avoided.

Keywords

Keywords (up to 10) should be listed immediately after the abstract; abbreviations should be used only if they are generally accepted and well-known in the field of research.

Division into chapters

The manuscript should be divided into chapters and sub-chapters, which are hierarchically numbered with Arabic numbers. The headings of chapters and sub-chapters should appear on their own separate lines.

At the end of the manuscript, and before the references, it is obligatory to list the following statements:

CRediT authorship contribution statement

For transparency, we require corresponding authors to provide co-author contributions to the manuscript using the relevant CRediT roles. The CRediT taxonomy includes 14 different roles describing each contributor's specific contribution to the research output. The roles are: Conceptualization; Data curation; Formal analysis; Funding acquisition; Investigation; Methodology; Project administration; Resources; Software; Supervision; Validation; Visualization; Roles/Writing - original draft; and Writing - review & editing. Note that not all roles may apply to every manuscript, and authors may have contributed through multiple roles.

Declaration of competing interest

Corresponding authors, on behalf of all the authors of a submission, must disclose any financial and personal relationships with other people or organizations that could inappropriately influence their work. Examples of potential conflicts of interest include employment, consultancies, stock ownership, honoraria, paid expert testimony, patent applications/registrations, and grants or other funding. All authors, including those *without* competing interests to declare, should provide the relevant information to the corresponding author (which, where relevant, may specify they have nothing to declare).

Declaration of generative AI in scientific writing

This guidance only refers to the writing process, and not to the use of AI tools to analyze and draw insights from data as part of the research process. Where authors use generative artificial intelligence (AI) and AI- assisted technologies in the writing process, authors should only use these technologies to improve readability and language. Applying the technology should be done with human oversight and control, and authors should carefully review and edit the result, as AI can generate authoritative-sounding output that can be incorrect, incomplete or biased. AI and AI-assisted technologies should not be listed as an author or co-author, or be cited as an author. Authorship implies responsibilities and tasks that can only be attributed to and performed by humans. Authors should disclose in their manuscript the use of AI and AI- assisted technologies in the writing process by following the instructions below. A statement will appear in the published work. Please note that authors are ultimately responsible and accountable for the contents of the work.

Disclosure instructions

Authors must disclose the use of generative AI and AI-assisted technologies in the writing process by adding a statement at the end of their manuscript in the core manuscript file, before the References list. The statement should be placed in a new section entitled 'Declaration of Generative AI and AI-assisted technologies in the writing process'.

Statement: During the preparation of this work the author(s) used [NAME TOOL / SERVICE] in order to [REASON]. After using this tool/service, the author(s) reviewed and edited the content as needed and take(s) full responsibility for the content of the publication.

This declaration does not apply to the use of basic tools for checking grammar, spelling, references etc. If there is nothing to disclose, there is no need to add a statement.

Acknowledgments

State the institutions and persons who financially or in some other way helped the presented research. If the research was not supported by others, it should also be stated in this part of the manuscript.

Appendices

The manuscript may have appendices. If there is more than one appendix, they are denoted by A, B, etc. Labels of figures, tables and formulas in appendices should contain the label of the appendix, for example Table A.1, Figure A.1, etc.

ABBREVIATIONS

All abbreviations should be defined where they first appear. Consistency of abbreviations used throughout the text should be ensured.

MATH FORMULAE

Formulae should be in the form of editable text (not in the format of figures) and marked with numbers, in the order in which they appear in the text. The formulae and equations should be written carefully taking into account the indices and exponents. Symbols in formulae should be defined in the order they appear, right below the formulae.

FIGURES

- figures should be made so that they are as uniform in size as possible and of appropriate quality for reproduction;
- the dimensions of the figures should correspond to the format of the journal: figures with a width approximately equal to the width of 1 column (± 80 mm width), width of 2 columns (± 170 mm width) or width of 1.5 columns (± 130 mm width);
- figures should be designed so that their size is not disproportionately large in relation to the content;
- the text on the figures should be minimal and the font used should be the same on all figures (Arial, Times New Roman, Symbol);
- figures should be placed next to the appropriate text in the manuscript and marked with numbers in the order in which they appear in the text;
- each figure should have a caption that is placed below the figure - the caption should not be on the figure itself.
  In cases of inadequate quality of reproduction, the author should be required to submit figures as separate files. In this case, the figure should be saved in TIFF (or JPG) format with a minimum resolution of 500 dpi.

TABLES

- tables should be in the form of editable text (not in the format of figures);
- tables should be placed next to the appropriate text in the manuscript and marked with numbers in the order in which they appear in the text;
- each table should have a caption that is placed below the table;
- the tables should not show the results that are already presented elsewhere in the manuscript - duplicating the presentation of results should be avoided;
- tables are without vertical lines as boundaries between cells and shading cells.

REFERENCES

Citation in the text

Each reference cited in the text should be in the reference list (and vice versa). It is not recommended to list unpublished results or personal communications in the reference list, but they can be listed in the text. If they are still listed in the reference list, the journal style references are used, with 'Unpublished results' or 'Personal communication' instead of the date of publication. Citing a reference as 'in press' means that it is accepted for publication.

Web references

Web references are minimally listed with the full URL and the date when the site was last accessed. These references can be included in the reference list, but can also be given in a separate list after the reference list.

Reference style

In text: References are given in the text by a number in square brackets in the order in which they appear in the text. Authors may also be referred to directly, but the reference number should always be given.

In reference list: References marked with a number in square brackets are sorted by numbers in the list.

Examples

Reference to a journal publication:

[1] V.W.Y. Tam, M. Soomro, A.C.J. Evangelista, A review of recycled aggregate in concrete applications (2000-2017), Constr. Build. Mater. 172 (2018) 272-292. https://doi.org/10.1016/j.conbuildmat.2018.03.240.

Reference to a book:

[3] A.H. Nilson, D. Darwin, C.W. Dolan, Design of Concrete Structures, thirteenth ed., Mc Graw Hill, New York, 2004.

Reference to a chapter in an edited book:

[4] J.R. Jimenez, Recycled aggregates (RAs) for roads, in: F Pacheco-Torgal, V.W.Y. Tam, J.A. Labrincha, Y. Ding, J. de Brito (Eds.), Handbook of recycled concrete and demolition waste, Woodhead Publishing Limited, Cambridge, UK, 2013, pp. 351–377.

Reference to a website:

[5] WBCSD, The Cement Sustainability Initiative, World. Bus. Counc. Sustain. Dev. http://www.wbcsdcement.org.pdf/CSIRecyclingConcrete-FullReport.pdf, 2017 (accessed 7 July 2016).

SUPPLEMENTARY MATERIAL

Supplementary material such as databases, detailed calculations and the like can be published separately to reduce the workload. This material is published 'as received' (Excel or PowerPoint files will appear as such online) and submitted together with the manuscript. Each supplementary file should be given a short descriptive title.

ETHICS IN PUBLISHING

Authors are expected to respect intellectual and scientific integrity in presentation of their work. The journal publishes manuscripts that have not been previously published and are not in the process of being considered for publication elsewhere. All co-authors as well as the institution in which the research was performed should agree to the publication in the journal.
Authors are expected to submit completely original research; if the research of other researchers is used, it should be adequately cited. Authors who wish to include in their manuscript images, tables or parts of text that have already been published somewhere, should obtain permission from the Copyright owner and provide a proof in the process of submitting the manuscript. All material for which there is no such evidence will be considered the original work of the author. To determine the originality of the manuscript, it can be checked using the Crossref Similarity Check service. For more information, please see our Ethics and Malpractice Statement.

The Journal and Publishers imply that all authors, as well as responsible persons of the institute where the research was performed, agreed with the content of the submitted manuscript before submitting it. The Publishers will not be held legally responsible should there be any claims for compensation.

PEER REVIEW

This journal uses a single blind review process, which means that the authors do not know the names of the reviewers, but the reviewers know who the authors are. In the review process, the Editor-in-Chief first assesses whether the contents of the manuscript comply with the scope of the journal. If this is the case, the paper is sent to at least two independent experts in the field, with the aim of assessing its scientific quality and making recommendation regarding publication. If the manuscript needs to be revised, the authors are provided with the reviewers' remarks. The authors are obliged to correct the manuscript in accordance with the remarks, submit the revised manuscript and a special file with the answers to the reviewers within the given deadline. The final decision, whether the paper will be published in journal or not, is made by the Editor-in-Chief.

AFTER ACCEPTANCE

Once accepted for publication, the manuscript is set in the journal format. Complex manuscript is sent to the authors in the form of proof, for proof reading. Then, authors should check for typesetting errors, and whether the text, images, and tables are complete and accurate. Authors are asked to do this carefully, as subsequent corrections will not be considered. In addition, significant changes to the text and authorship at this stage are not allowed without the consent of the Editor-in-Chief. After online publication, changes are only possible in the form of Erratum which will be hyperlinked to manuscript.

COPYRIGHT

Authors retain copyright of the published papers and grant to the publisher the non-exclusive right to publish the article, to be cited as its original publisher in case of reuse, and to distribute it in all forms and media.

The published articles will be distributed under the Creative Commons Attribution ShareAlike 4.0 International license (CC BY-SA). It is allowed to copy and redistribute the material in any medium or format, and remix, transform, and build upon it for any purpose, even commercially, as long as appropriate credit is given to the original author(s), a link to the license is provided, it is indicated if changes were made and the new work is distributed under the same license as the original.

Users are required to provide full bibliographic description of the original publication (authors, article title, journal title, volume, issue, pages), as well as its DOI code. In electronic publishing, users are also required to link the content with both the original article published in *Building Materials and Structures* and the license used.

Authors are able to enter into separate, additional contractual arrangements for the non-exclusive distribution of the journal's published version of the work (e.g., post it to an institutional repository or publish it in a book), with an acknowledgement of its initial publication in this journal.

OPEN ACCESS POLICY

Journal *Building Materials and Structures* is published under an Open Access license. All its content is available free of charge. Users can read, download, copy, distribute, print, search the full text of articles, as well as to establish HTML links to them, without having to seek the consent of the author or publisher.
The right to use content without consent does not release the users from the obligation to give the credit to the journal and its content in a manner described under *Copyright*.

Archiving digital version

In accordance with law, digital copies of all published volumes are archived in the legal deposit library of the National Library of Serbia in the Repository of SCIndeks - The Serbian Citation Index as the primary full text database.

Cost collection to authors

Journal Building Materials and Structures does not charge authors or any third party for publication. Both manuscript submission and processing services, and article publishing services are free of charge. There are no hidden costs whatsoever.

DISCLAIMER

The views expressed in the published works do not express the views of the Editors and the Editorial Staff. The authors take legal and moral responsibility for the ideas expressed in the articles. Publisher shall have no liability in the event of issuance of any claims for damages. The Publisher will not be held legally responsible should there be any claims for compensation.

Financial support